© 2024. Published by The Company of Biologists Ltd | Journal of Experimental Biology (2024) 227, jeb247434. doi:10.1242/jeb.247434

RESEARCH ARTICLE

SPECIAL ISSUE
THE INTEGRATIVE BIOLOGY OF THE HEART

Developmental programming of sarcoplasmic reticulum function improves cardiac anoxia tolerance in turtles

Ilan M. Ruhr[1,2,*], Holly A. Shiels[1], Dane A. Crossley, II[3] and Gina L. J. Galli[1,*]

ABSTRACT

Oxygen deprivation during embryonic development can permanently remodel the vertebrate heart, often causing cardiovascular abnormalities in adulthood. While this phenomenon is mostly damaging, recent evidence suggests developmental hypoxia produces stress-tolerant phenotypes in some ectothermic vertebrates. Embryonic common snapping turtles (*Chelydra serpentina*) subjected to chronic hypoxia display improved cardiac anoxia tolerance after hatching, which is associated with altered Ca^{2+} homeostasis in heart cells (cardiomyocytes). Here, we examined the possibility that changes in Ca^{2+} cycling, through the sarcoplasmic reticulum (SR), underlie the developmentally programmed cardiac phenotype of snapping turtles. We investigated this hypothesis by isolating cardiomyocytes from juvenile turtles that developed in either normoxia (21% O_2; 'N21') or chronic hypoxia (10% O_2; 'H10') and subjected the cells to anoxia/reoxygenation, in either the presence or absence of SR Ca^{2+}-cycling inhibitors. We simultaneously measured cellular shortening, intracellular Ca^{2+} concentration ($[Ca^{2+}]_i$), and intracellular pH (pH_i). Under normoxic conditions, N21 and H10 cardiomyocytes shortened equally, but H10 Ca^{2+} transients ($\Delta[Ca^{2+}]_i$) were twofold smaller than those of N21 cells, and SR inhibition only decreased N21 shortening and $\Delta[Ca^{2+}]_i$. Anoxia subsequently depressed shortening, $\Delta[Ca^{2+}]_i$ and pH_i in control N21 and H10 cardiomyocytes, yet H10 shortening and $\Delta[Ca^{2+}]_i$ recovered to pre-anoxic levels, partly due to enhanced myofilament Ca^{2+} sensitivity. SR blockade abolished the recovery of anoxic H10 cardiomyocytes and potentiated decreases in shortening, $\Delta[Ca^{2+}]_i$ and pH_i. Our novel results provide the first evidence of developmental programming of SR function and demonstrate that developmental hypoxia confers a long-lasting, superior anoxia-tolerant cardiac phenotype in snapping turtles, by modifying SR function and enhancing myofilament Ca^{2+} sensitivity.

KEY WORDS: Cardiomyocyte, Developmental hypoxia, Developmental plasticity, Ectotherm, Ca^{2+} cycling, Phenotypic plasticity

[1]Division of Cardiovascular Sciences, School of Medical Sciences, University of Manchester, Manchester M13 9NT, UK. [2]School of Science, Engineering, & Environment, University of Salford, Salford M5 4NT, UK. [3]Department of Biological Sciences, University of North Texas, Denton, TX 76203, USA.

*Authors for correspondence (i.m.ruhr@salford.ac.uk; gina.galli@manchester.ac.uk)

I.M.R., 0000-0001-9243-7055; H.A.S., 0000-0001-5223-5205; D.A.C., 0000-0001-9683-7013; G.L.J.G., 0000-0002-1023-915X

Received 1 February 2024; Accepted 27 August 2024

INTRODUCTION

The environment an organism experiences during embryonic or fetal development has a powerful, and often permanent, influence over its phenotype (Moczek, 2015). This phenomenon, termed developmental plasticity, can result in individuals that share a single genotype displaying substantially different phenotypes, depending on the developmental environment (Bateson et al., 2014). Developmental processes are susceptible to oxygen availability, and a lack of oxygen (hypoxia) during development is a particularly potent stressor that can affect multiple organ systems and alter the developmental trajectory of vertebrates (Burggren and Reyna, 2011). In the cardiovascular system, developmental hypoxia has a profound, life-long impact, which, for fetal mammals and birds, leads to remodelling that produces maladaptive phenotypes and predisposes individuals to disease susceptibility in adulthood (Giussani, 2021). Interestingly, recent evidence suggests developmental hypoxia might improve cardiovascular outcomes in some ectothermic vertebrates (Galli et al., 2023). Accordingly, understanding the mechanisms that programme adaptive cardiovascular phenotypes in ectothermic vertebrates has broad ecological and clinical implications.

As with many North American freshwater turtles, the developmental environment of common snapping turtles (*Chelydra serpentina*) is characterised by routine fluctuations in oxygen (Ackerman and Lott, 2004; Ultsch, 2006). Turtles are oviparous ectotherms, and lay their eggs in subterranean nests, which can become chronically hypoxic, depending on factors that include nest depth, egg metabolic activity, microbial respiration and flooding (Ackerman and Lott, 2004). Consequently, eggs laid in the deepest part of a nest might experience O_2 tensions as low as 10%, whereas eggs at the surface have access to atmospheric tensions of up to 21% O_2 (Ackerman and Lott, 2004; Booth, 2000). Based on mammalian and avian outcomes (Galli et al., 2023), such dramatic differences in developmental oxygen are expected to severely alter the turtle cardiovascular system. Indeed, numerous studies show that embryonic turtles respond to hypoxia very similarly to mammals and birds, with long-lasting alterations to cardiovascular form and function (Eme et al., 2014, 2013, 2021; Sartori et al., 2019; Tate et al., 2015). However, unlike mammals and birds, these changes appear to enhance aspects of cardiovascular performance after hatching in juvenile snapping turtles (Ruhr et al., 2021; Smith et al., 2022; Wearing et al., 2017, 2016). The most distinguishing feature of the hypoxia-programmed turtle heart is its extreme tolerance to anoxia. Snapping turtles from hypoxic incubations maintain cardiac power output and heart rate roughly twofold higher than individuals from normoxic incubations, even during 2 h in anoxic conditions (Ruhr et al., 2021). Hypoxia presumably acts as an external cue that primes an embryonic snapping turtle's physiology to a future life in low-oxygen habitats or activities (e.g. diving underwater for extended periods to forage, thermoregulate or escape a threat). When

Journal of Experimental Biology (2024) 227, jeb247434. doi:10.1242/jeb.247434

underwater, freshwater turtles routinely engage in breath-hold dives, during which they are subjected to bouts of hypoxia (Gatten, 1980; Jackson and Silverblatt, 1974). Improved cardiac function, by previous exposure to developmental hypoxia, could conceivably provide an advantage by more rapidly delivering O_2/nutrients to the muscles and removing of CO_2/wastes from the tissues, thereby enhancing underwater performance. Considering that wild freshwater turtles actively exploit oxygen-deprived environments and overwinter in anoxic, ice-covered lakes throughout their lives (Jackson, 2000; Ultsch, 2006), the programming of cardiac anoxia tolerance could be beneficial for their future survival in hypoxic environments.

Developmental programming typically occurs by epigenetic modifications, whereby DNA is differentially methylated, and these changes can persist throughout the life of an individual (Hanson et al., 2014). We have recently begun to unravel the mechanisms underlying the programming of cardiac anoxia tolerance in snapping turtles, and found evidence of adaptive plasticity at the cellular (Ruhr et al., 2019), metabolic (Galli et al., 2021) and molecular (Ruhr et al., 2021) levels. We showed that the remarkable anoxia tolerance of the juvenile turtle heart is apparent in isolated cardiac cells (cardiomyocytes), which is supported by enhanced myofilament calcium (Ca^{2+}) sensitivity and low basal production of reactive oxygen species (ROS) (Ruhr et al., 2019). These adaptive phenotypes are associated with changes in gene expression and the differential methylation of genes linked to cardiomyocyte excitation and contraction (Ruhr et al., 2021). Curiously, we revealed that ventricular cardiomyocytes isolated from snapping turtles previously exposed to developmental hypoxia had much smaller Ca^{2+} transients than their normoxic counterparts (Ruhr et al., 2019). This finding suggests that Ca^{2+}-cycling pathways and/or Ca^{2+}-storage sites in ventricular cardiomyocytes have been permanently modified by developmental hypoxia. Thus, it is possible that modifications to intracellular Ca^{2+} handling could be partly responsible for the programming of turtle cardiac anoxia tolerance.

Maintenance of excitation–contraction (EC) coupling within cardiomyocytes is critically important to surviving hypoxia. Briefly, an action potential initiates the opening of sarcolemmal L-type Ca^{2+} channels that triggers an influx of extracellular Ca^{2+} (I_{Ca}), which causes a larger release of Ca^{2+} stored in the sarcoplasmic reticulum (SR) through ryanodine receptors (RyRs) (Bers, 2002). This process, termed Ca^{2+}-induced Ca^{2+} release, culminates in a rise of cytosolic free Ca^{2+} concentration ($[Ca^{2+}]_i$). The Ca^{2+} then acts as a secondary messenger that binds to troponin-C on the myofilaments, leading to cross-bridge cycling and cardiomyocyte contraction (Gillis, 2011). During relaxation, Ca^{2+} is either pumped back into the SR, through the SR Ca^{2+}-ATPase (SERCA) or transported across the sarcolemma, through the Na^+/Ca^{2+}-exchanger (NCX) (Bers, 2002). The magnitude of the rise in $[Ca^{2+}]_i$ – the Ca^{2+} transient ($\Delta[Ca^{2+}]_i$) – is the chief regulator of contractile force (Bers, 2002).

While EC coupling is a ubiquitous and conserved process among vertebrate classes, there are substantial differences in the ways species cycle Ca^{2+} during contraction and relaxation. Mammals rely heavily on the SR for Ca^{2+} cycling, but ectothermic vertebrates typically possess poorly developed cardiac SR (Bossen and Sommer, 1984; Lillywhite et al., 1999) and rely almost exclusively on trans-sarcolemmal Ca^{2+} flux for contraction and relaxation (Cros et al., 2014; Shiels and Galli, 2014; Shiels et al., 2002b; Vornanen et al., 2002), rather than SR Ca^{2+} release (Tibbits et al., 1990). However, exceptions exist in nature, and it is thought that SR Ca^{2+} cycling is more prevalent in physically active species of ectotherms (Galli et al., 2009a,b; Keen et al., 1992; Shiels et al., 2011, 1999; Shiels and Farrell, 2000) and also maintains cardiac contractility during environmental stress (Kubly and Stecyk, 2019; MacCormack et al., 2003; Shiels and Farrell, 1997). This can occur through many mechanisms, including changes in SR structural organisation, SR density and the expression of SR proteins (e.g. RyR and SERCA). The sensitivity of the myofilaments to Ca^{2+} is also increased by acute and chronic environmental stressors, leading to enhanced contractility (Churcott et al., 1994; Fanter et al., 2017; Klaiman et al., 2014; Ruhr et al., 2019). Mechanisms that increase myofilament Ca^{2+} sensitivity include an increase in pH, reduced adrenergic tone and changes in the abundance or activity of myofilament proteins, such as troponin and myosin (Chung et al., 2016). These earlier studies suggest that modulation of pathways involved in SR Ca^{2+} cycling and myofilament Ca^{2+} sensitivity could play a role in the programming of cardiac anoxia tolerance in turtles.

Although North American freshwater turtles are relatively sedentary and are usually reliant on cardiomyocyte sarcolemmal Ca^{2+} cycling, we propose that developmental hypoxia could permanently alter cardiac SR function in turtles, leading to improved anoxia tolerance. Therefore, in this study, we determined the functional contribution of SR Ca^{2+} cycling during anoxia and reoxygenation in ventricular cardiomyocytes from juvenile common snapping turtles that were previously incubated in either normoxia (21% O_2) or chronic hypoxia (10% O_2) during embryonic development. To our knowledge, we provide the first evidence of developmental plasticity of cardiac SR function. We also demonstrate that freshwater turtles depend on the SR when the heart is challenged by anoxia, highlighting the importance of SR Ca^{2+} cycling (rather than transarcolemmal Ca^{2+} transport) that is observed in the stressed hearts of other vertebrate species (Shiels and Galli, 2014).

MATERIALS AND METHODS

Turtle collection

Eggs from multiple clutches of common snapping turtles, *Chelydra serpentina* (Linnaeus 1758), were collected from the wild, in Minnesota, USA, and transported for incubation to the University of North Texas (Denton, TX, USA). Permission to collect the eggs was granted to D.A.C. by the Minnesota Department of Natural Resources (permit no. 21232). Two eggs from each clutch were staged to determine embryonic age. All eggs were artificially incubated by embedding them to their midpoint in vermiculite, inside plastic incubators (2.5-L Ziploc Container, SC Johnson, Racine, WI, USA) that were stored in a walk-in Environmental Control Room (model IR-912L5, Percival Scientific, Perry, IA, USA). The vermiculite was mixed in a 1:1 ratio with water, as previously described (Crossley and Altimiras, 2005).

Turtle incubations

At approximately 20% development (9–12 days after laying; determined by embryonic staging), eggs were randomly assigned to two incubation groups: either normoxia (atmospheric 21% O_2) or hypoxia (10% O_2). Given that atmospheric gas composition is nominally 21% O_2 and to distinguish between the experimental oxygen treatment of normoxia, individuals that were incubated in 21% O_2 are denoted as ‘N21’, while those incubated in 10% O_2 are denoted as ‘H10’. These oxygen levels were chosen because they occur naturally in wild turtle nests (Ackerman and Lott, 2004) and produce distinct whole-organ, cellular, metabolic, transcriptomic and methylomic cardiac phenotypes in juvenile and adult snapping turtles (Galli et al., 2021; Ruhr et al., 2021, 2019; Wearing et al., 2017; Wearing et al., 2016).

Because sex determination in turtles is dependent on embryonic temperature, all eggs were incubated at a female-determining 30°C

(Alvine et al., 2013; Yntema, 1968). To achieve the desired oxygen levels, parallel gas inflow and outflow tubes were attached to the incubators, and gas mixtures were set to a flow rate of 2–3 l min^{-1} using rotameters (Sho-Rate Brooks Instruments Division, Hatfield, PA, USA); room air was used for the N21 incubations and a compressed-N_2/room-air mixture was used for the H10 incubations. The gas mixtures passed through an H_2O bubbler to ensure 80–95% relative humidity, and their compositions were monitored continuously with an oxygen analyser (S-3AI, AEI Technologies, Pittsburgh, PA, USA). The eggs began to hatch approximately 55 days after they were laid; thus, the duration of the incubations was between 43 and 46 days.

Turtle husbandry

Upon hatching, all turtles were housed in the common-garden conditions of 21% O_2 and 26°C. Turtles were fed dry crocodilian food (Mazuri, PMI Nutrition International, Brentwood, MO, USA) 2–4 times weekly *ad libitum*, kept on a daily 12 h:12 h light:dark cycle, and provided with both distilled water and basking areas. At 7 months post-hatch, the hatchlings were transported by air-freight to the University of Manchester (Manchester, UK), where they were individually housed in 21% O_2 and 26°C, kept on a daily 12 h:12 h light:dark cycle, and fed fresh krill and Tetra ReptoMin (Spectrum Brands, Blacksburg, VA, USA), *ad libitum*, 3 times weekly. Turtle husbandry and experimental procedures were carried out in accordance with University of Manchester handling protocols, which adhere to the UK Home Office legislation. Experiments were carried out when the turtles reached a juvenile age, between 15 and 24 months; N21 turtles weighed (mean±s.e.m.) 314.8±27.4 g (range: 113–477 g) and H10 turtles weighed 717.4±46.7 g (range: 375–984 g), with no significant differences in body mass between the two groups.

Cardiomyocyte isolation

Ventricular cardiomyocytes were isolated by enzymatic dissociation, as previously described (Galli et al., 2006b; Ruhr et al., 2019). Briefly, turtles were killed by rapid decapitation; the brain and spinal cord were destroyed by pithing and the head was flash frozen in liquid nitrogen. The heart was quickly excised and cannulated by retrograde perfusion, through the aortic arch into the ventricle. The ventricle was initially perfused with isolation solution for 8–10 min (to remove blood, debris, Ca^{2+} and other blood-plasma ions) and then with enzymatic dissociation solution for 26–30 min (see Table 1 for solution compositions). Solutions were heated to between 28 and 30°C, with an In-line Heater/Cooler Peltier (model SC-20, Warner Instruments, Hamden, CT, USA), connected to a Single-Channel Temperature Controller (model TC-324C, Warner Instruments). After perfusion, the ventricle was removed and minced into small pieces (≤3 mm), and individual ventricular cardiomyocytes were released by gentle agitation. Finally, cardiomyocytes were suspended in isolation solution and stored at 4°C, for up to 8 h. A total of 25 juvenile turtles were used in this study (N=14 and 11 individuals from normoxic and hypoxic incubations, respectively), and their body and heart masses are recorded in Table S1.

Perfusion saline solutions

The composition of all saline solutions used in this study is provided in Table 1. To our knowledge, the concentration of plasma ions of snapping turtles in normoxia or anoxia has not been determined experimentally, at room temperature (20–22°C). Therefore, our saline solutions were designed according to ion concentrations measured in the plasma of red-eared slider turtles (*Trachemys scripta*) breathing 21% O_2, at 25°C (Warren and Jackson, 2007), which we used in a previous study (Ruhr et al., 2019). To reveal differences in anoxia tolerance between the N21 and H10 cardiac phenotypes, we subjected the isolated cardiomyocytes to an anoxic saline that combined three main elements of *in vivo* anoxia: zero oxygen, CO_2 retention and lactate build-up. The precise values of dissolved gases and ion concentrations in plasma were also based on those in *T. scripta*, after 4 h of anoxia, at 25°C (Warren and Jackson, 2007). While the concentrations of other plasma ions change with *in vivo* anoxia (e.g. Ca^{2+}, Mg^{2+} and K^+), we limited changing some variables for our simulated anoxic challenge to facilitate the interpretation of phenotypic differences between N21 and H10 cardiomyocytes. All chemicals were purchased from Sigma-Aldrich, unless otherwise stated.

Experimental equipment

We used epifluorescent microscopy to simultaneously measure cardiomyocyte shortening, intracellular [Ca^{2+}] ($[Ca^{2+}]_i$), and intracellular pH (pH_i), during three distinct experimental oxygen periods: normoxia, an anoxic challenge and reoxygenation (Fig. S1A). The isolated cardiomyocytes were placed in a perfusion bath (model Series RC-21BRFS, Warner Instruments; Fig. S1B) with built-in field-stimulation electrodes, which were connected to a stimulator (model SD-9, Grass Instruments, Astro-Med, Inc., West Warwick, RI, USA). The perfusion bath was inserted into a custom-built environmental chamber (Bold-Line Top Stage Incubator, model H301-NIKON-TI-SR, Okolab, Ottaviano, NA, Italy; Fig. S1C), into which an oxygen probe was inserted (mini-sensor model TROXF1100 and FireStingO_2 optical oxygen meter, PyroScience GmbH, Aachen, Germany; Fig. S1C). Gas-tight perfusion lines were also inserted into the chamber and were connected to external gas cylinders. Epifluorescence images of the cardiomyocytes were recorded by mounting the environmental chamber onto an inverted microscope (model Eclipse TE-2000U, Nikon, Surbiton, UK) that was coupled to an Optoscan photomultiplier tube, a monochromator and a high-intensity xenon arc lamp (Cairn Research Instruments, Faversham, UK). Signals were digitised with a Digidata 1440A and analysed with pClamp software (v10.7, Axon Instruments, Sunnyvale, CA, USA).

Fluorescent indicators and inhibitors

To measure $[Ca^{2+}]_i$ and pH_i simultaneously, resuspended cardiomyocytes were co-loaded with the acetoxymethyl (AM)-ester, cell-permeant fluorescent indicators Fura-2 AM and BCECF AM [2′,7′-bis(2-carboxyethyl)-5(6)-carboxyfluorescein AM; Invitrogen, Loughborough, UK), respectively, at room temperature. Cells were loaded with the indicators by co-incubating them with Fura-2 (0.075 µmol l^{-1}), for 10 min, and BCECF (0.8 µmol l^{-1}), for 30 min. To prevent leakage across the plasma membrane, we de-esterified the indicators, by resuspending the cells in fresh isolation solution, for 15–20 min. To inhibit SR Ca^{2+} cycling, a subset of resuspended cells was co-incubated with ryanodine (10 µmol l^{-1}; a RyR blocker) and thapsigargin (2 µmol l^{-1}; a SERCA blocker), for 30 min, at room temperature.

Simulated anoxia and reoxygenation protocol

Following the loading protocol, cardiomyocytes were placed in the recording chamber (at room temperature), perfused with normoxic saline, and stimulated to contract at the physiologically relevant frequency of 0.2 Hz (Frische et al., 2000; Ruhr et al., 2021; Wearing et al., 2017). After a 10 min stabilisation period, the perfusate was switched to the anoxic saline, for 20 min, and cells were subsequently reoxygenated by switching back to the normoxic saline, for a further 10 min (Fig. S1A). Oxygen was measured continuously with the FireStingO_2 probe throughout the protocol and was undetectable during the anoxic period. We note that measurements were taken at a

Journal of Experimental Biology (2024) 227, jeb247434. doi:10.1242/jeb.247434

Table 1. Composition of solutions used in the present study

	Heart-perfusion solutions		Experimental saline solutions		Calibration solutions	
Component	Isolation	Dissociation§	Normoxia¶	Anoxia‡	BCECF	Fura-2#
NaCl (mmol l^{-1})	100	100	95	82		95
KCl (mmol l^{-1})	10	10	2.9	2.9	140	2.9
$NaHCO_3$ (mmol l^{-1})			35	15		
Na_2HPO_4 (mmol l^{-1})			0.74	0.74		0.74
NaH_2PO_4 (mmol l^{-1})			0.6	0.6		0.6
KH_2PO_4 (mmol l^{-1})	1.2	1.2				
$MgCl_2$ (mmol l^{-1})			1.2	1.2	1	1.2
$MgSO_4$ (mmol l^{-1})	4	4				
$CaCl_2$ (mmol l^{-1})			2	2		2#
Sodium lactate (mmol l^{-1})				30		
Hepes (mmol l^{-1})	10	10			10	10
Taurine (mmol l^{-1})	50	50				
Glucose (mmol l^{-1})	20	20	5	5	8	5
EGTA (mmol l^{-1})					1	10#
Nigericin (μmol l^{-1})					7	
Rotenone (μmol l^{-1})						2
Iodoacetate (mmol l^{-1})						5
CCCP (μmol l^{-1})						5
Ionomycin (μmol l^{-1})						10
Trypsin (mg ml^{-1})		0.5				
Collagenase (mg ml^{-1})		0.75				
BSA (mg ml^{-1})		0.75				
$O_2/CO_2/N_2$ (%)			21/3/76	0/11/89		
pH	6.9*	6.9*	7.72¶	6.8‡	6.5, 7, 7.5, 8*	7.7*

§Enzymes were dissolved in the solution, just prior to enzymatic perfusion; ¶saline was equilibrated with a gas mixture of 3% CO_2, 21% O_2 and 76% N_2, to yield a pH of 7.72 in solution; ‡saline was equilibrated with a gas mixture of 11% CO_2 and 89% N_2, to yield a pH of 6.8 in solution; #two solutions were used to calibrate Fura-2 (one contained EGTA and the other contained $CaCl_2$), as described in detail in Materials and Methods; *pH adjusted with KOH.

common frequency of 0.2 Hz throughout the experimental protocol (i.e. normoxia, anoxia and reoxygenation). This is a limitation to our study, given that turtles experience a profound bradycardia during anoxia (Jackson, 2000). Therefore, the effects of anoxia on cellular shortening and SR Ca^{2+} cycling might have been different at lower frequencies.

Measurement of $[Ca^{2+}]_i$ and pH_i

All excitation light waves were filtered with a Nikon T510lpxru dichroic (Chroma Technology Corp, Olching, Germany) long-pass filter and emitted light waves were collected using a HQ535/50 m filter (Chroma) to capture Fura-2 and BCECF emissions. Fura-2 and BCECF were excited sequentially with 340 nm/380 nm and 490 nm/440 nm wavelengths, respectively, and light was collected at 515 nm. Fura-2 input and exit slit widths were each set to 10 nm and BCECF slit widths were set to 7 nm (input) and 4 nm (exit). Fura-2 and BCECF were calibrated using previously published protocols (James-Kracke, 1992; Lattanzio, 1990; Shiels et al., 2002a).

For the BCECF calibration, cells were perfused with a series of solutions of increasing pH (6.5 to 8.0) that contained nigericin (7 μmol l^{-1}), a K^+ ionophore (Table 1). A four-step pH calibration was used to generate a standard curve, in which the fluorescence output measurements were converted into pH_i.

For the Fura-2 calibration, cells were perfused with an extracellular solution (Table 1) that contained the metabolic inhibitors rotenone (2 μmol l^{-1}), sodium iodoacetate (5 μmol l^{-1}), carbonyl cyanide 3-chlorophenylhydrazone (5 μmol l^{-1}; prevents Ca^{2+} sequestration in the mitochondria), and ionomycin (10 μmol l^{-1}; a Ca^{2+} ionophore). To measure maximum (R_{max}) and minimum (R_{min}) Ca^{2+} fluorescence (see below), EGTA (10 mmol l^{-1}; a Ca^{2+}-chelating agent) and $CaCl_2$ (2 mmol l^{-1}) were added to the extracellular solution, respectively.

The collected 340 nm/380 nm ratiometric data were converted to $[Ca^{2+}]_i$, using Fura-2 dissociation constants (K_d) and the equation previously described by Lattanzio (1990). Briefly, K_d values were derived from a Ca^{2+}-binding standard curve for Fura-2, using solutions of decreasing pH (7.4 to 5.5, at 22°C) and by producing a best-fit curve, which shows a gradually lower Ca^{2+}-binding affinity (i.e. a higher K_d) with decreasing pH. Finally, $[Ca^{2+}]_i$ was calculated with the following formula (Lattanzio, 1990):

$$[Ca^{2+}]_i = K_d \times [(R - R_{min})/(R_{max} - R)] \times (S_{f_2}/S_{b_2}), \quad (1)$$

where K_d is the dissociation constant (a measure of binding affinity); R is the measured 340 nm/380 nm ratio of Fura-2 fluorescence within a cell; R_{min} and R_{max} are the fluorescence ratios of the calcium-free and fully calcium-bound Fura-2, respectively; and S_{f_2} and S_{b_2} are the 380 nm fluorescence values of calcium-free and fully calcium-bound Fura-2, respectively.

Measurement of cardiomyocyte shortening

A high-resolution, infra-red camera (model 902B EIA, Watec, Newburgh, NY, USA) was connected to the Nikon microscope and recorded cardiomyocyte contractions. Cardiomyocyte contractions were collected concurrently with Fura-2 fluorescence, recorded onto DVDs and analysed using the open-source software CellX (https://github.com/jake-rigby/CellX/releases/tag/v1.0.3). CellX allows relaxed and shortened cell length to be accurately measured, but does not have the resolution to faithfully record the kinetics of cellular contraction and relaxation.

Calculations and statistical analysis

GraphPad Prism (v10, GraphPad Software, Boston, MA, USA) and SPSS (v29, IBM, Armonk, NY, USA) were used for figure

production and statistical analyses, respectively. Data were tested for equal variances and normality.

Generalised linear models (GLMs), followed by Šidák *post hoc* tests (for multiple comparisons), were used to determine differences in body mass, heart mass and heart-to-body-mass ratios. For these GLMs, the fixed factor was embryonic oxygen. The data for body and heart mass were normally distributed, but those for the heart-to-body-mass ratios were not. Thus, we fitted the mass data to normal distributions, while we log-transformed the ratio data and fitted them to a gamma distribution.

Repeated-measures, generalised linear mixed-effects models (GLMMs), followed by sequential Šidák *post hoc* tests, were used to determine differences in cardiomyocyte shortening, Ca^{2+} transients ($\Delta[Ca^{2+}]_i$), normalised $\Delta[Ca^{2+}]_i$, diastolic $[Ca^{2+}]_i$, systolic $[Ca^{2+}]_i$, pH_i, and kinetics (times to rise and half-decay). When analysing the anoxia/reoxygenation protocol, the GLMM fixed factors were embryonic oxygen incubation [21% O_2 (normoxia) and 10% O_2 (hypoxia)], inhibitor treatment (ryanodine and thapsigargin, to inhibit SR Ca^{2+} cycling), experimental oxygen/time. Because the data for all variables were not normally distributed, we transformed the data using either log or square-root functions and fitted them to normal or gamma distributions, depending on which model provided the best fit (Bolker, 2015), as indicated by Akaike's information criterion (AIC). $\Delta[Ca^{2+}]_i$ was calculated by subtracting the value of the diastolic $[Ca^{2+}]_i$ from the systolic $[Ca^{2+}]_i$.

Finally, to determine the effects of developmental hypoxia, SR inhibition and experimental oxygen on myofilament Ca^{2+} sensitivity, regression analyses and GLMMs were conducted on log- or square-root-transformed data. There were two sets of initial analyses: first, to determine experimental oxygen-dependent effects (i.e. N21 normoxia versus anoxia versus reoxygenation and H10 normoxia versus anoxia versus reoxygenation) and, second, both developmental and experimental oxygen-dependent effects (i.e. normoxia N21 versus H10, anoxia N21 versus H10, and reoxygenation N21 versus H10). The dependent variable was shortening, the fixed factors were experimental oxygen, developmental oxygen and SR inhibition, and the covariate was either $\Delta[Ca^{2+}]_i$ or pH_i. These initial analyses revealed that the slopes of the regressions did not differ between experimental oxygen treatments alone or when interacting with developmental oxygen. Thus, data were pooled to determine the effect of developmental hypoxia and SR inhibition, with shortening as the dependent variable, developmental oxygen and SR inhibition as the fixed factors, and $\Delta[Ca^{2+}]_i$ as the covariate.

All data are presented as means±s.e.m. and considered significantly different when $P \leq 0.05$. Note that the number of surviving cells is shown Table S2; survival was defined as cells not displaying alternans or not shrinking in size (due to cell death) during the experimental period.

RESULTS

Cardiac morphometrics

Although body and heart masses of turtles from normoxic and hypoxic incubations did not differ, developmental hypoxia resulted in a significantly higher heart-to-body-mass ratio and significantly shorter cardiomyocytes (Table 2).

Table 2. Morphometric measurements of body mass, heart mass, heart-to-body-mass, and isolated cardiomyocytes ratio from juvenile common snapping turtles that embryonically developed in normoxia (21% O_2; N21) or chronic hypoxia (10% O_2; H10)

	Developmental incubation	
Variable	N21	H10
Body mass (g)	314.79±27.41	263.91±36.43
Heart mass (mg)	717.44±46.73	676.05±72.88
Heart mass (mg):body mass (g) ratio	2.37±0.10	3.13±0.65*
Relaxed cell length (μm)	195.61±5.85	151.18±15.27*

Values are means±s.e.m., and statistical significance (*$P \leq 0.05$) between the normoxic (N=14) and hypoxic (N=11) incubation groups was revealed with generalised linear models, followed by one-tailed Šidák *post hoc* tests (for multiple comparisons).

Effects of developmental oxygen on the cardiomyocyte response to anoxia and reoxygenation

Representative traces of the effects of developmental hypoxia and inhibited SR Ca^{2+} cycling on the size, shape and duration of the $\Delta[Ca^{2+}]_i$ during simulated normoxia, anoxia and reoxygenation are shown in Fig. 1. The GLMs and GLMMs revealed significant effects of developmental oxygen, SR inhibition and experimental oxygen (i.e. anoxia and reoxygenation) on multiple aspects of juvenile turtle cardiomyocyte function. The significant effects of these experimental parameters are apparent in the size, shape and duration of $\Delta[Ca^{2+}]_i$ between the N21 and H10 groups (Fig. 1). F- and P-values for the fixed factors and their interactions are presented in Table 3, and full statistical results for the findings are given in Table S3 (i.e. test statistics, degrees of freedom and exact P-values).

Pre-anoxic (normoxic) conditions

Prior to anoxia exposure, there were no differences in shortening and pH_i between the control cardiomyocytes (i.e. non-SR-inhibited cells) of N21 and H10 juvenile turtles (Fig. 2). However, similar to our previous study (Ruhr et al., 2019), absolute $\Delta[Ca^{2+}]_i$ in N21 cells was more than twice the size of that in H10 cells (Fig. 2C,D). The large difference between $\Delta[Ca^{2+}]_i$ values was due to significantly lower H10 systolic $[Ca^{2+}]_i$ levels, whereas diastolic $[Ca^{2+}]_i$ levels were similar (Fig. 3). Although hypoxic development significantly reduced $\Delta[Ca^{2+}]_i$ in H10 cells, it had no impact on shortening.

SR Ca^{2+} cycling was inhibited with ryanodine and thapsigargin, which blocked the ryanodine Ca^{2+} channel and SERCA, respectively. Under normoxic conditions, SR inhibition significantly reduced cardiomyocyte shortening and $\Delta[Ca^{2+}]_i$ in N21 cells but not in H10 cells (Fig. 2A–D). Therefore, SR inhibition abolished the large difference in $\Delta[Ca^{2+}]_i$ between H10 and N21 control cells. The reduction in $\Delta[Ca^{2+}]_i$ for SR-inhibited N21 cells was due to changes in $[Ca^{2+}]_i$, in which diastolic $[Ca^{2+}]_i$ tended to rise and systolic $[Ca^{2+}]_i$ tended to fall, although these changes were not statistically significant (Fig. 3). The same pattern was observed in H10 cells; SR inhibition significantly decreased diastolic $[Ca^{2+}]_i$ at 10 min, but had no effect on systolic $[Ca^{2+}]_i$ (Fig. 3). SR inhibition also significantly hastened the time to half-decay in N21 and H10 cardiomyocytes, but did not alter the time to rise in either group (Tables 4 and 5). The overall effect of SR inhibition was a sharp reduction in shortening and $\Delta[Ca^{2+}]_i$ only in N21 cardiomyocytes, thereby demonstrating their reliance on SR Ca^{2+} cycling, under normoxic conditions, unlike H10 cells.

Anoxia and reoxygenation in control N21 and H10 cells

At the onset of the anoxic perfusion, oxygen rapidly dropped inside the environmental chamber to undetectable levels (<1 min), which had a significant negative inotropic effect on shortening in N21 and H10 cells (Fig. 2A,B), in association with significant reductions in $\Delta[Ca^{2+}]_i$ (Fig. 2C,D) and pH_i (Fig. 2G,H). However, while shortening in N21 cells remained depressed throughout the anoxic period, it recovered to pre-anoxic levels in H10 cells after 20 min of

Journal of Experimental Biology (2024) 227, jeb247434. doi:10.1242/jeb.247434

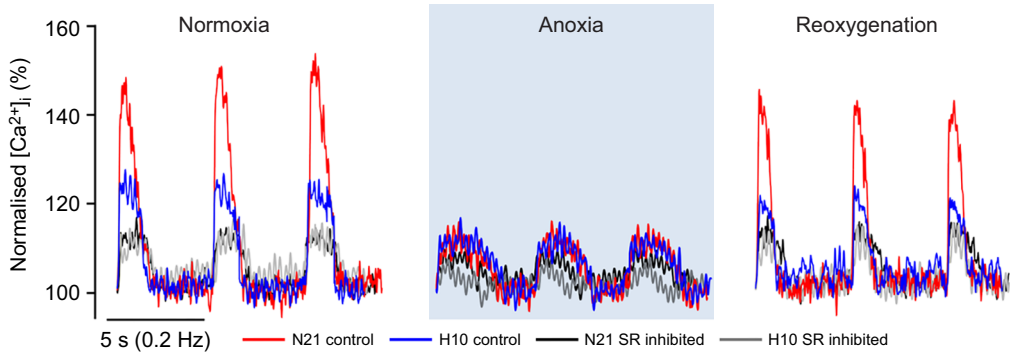

Fig. 1. Representative traces of the combined effects of developmental oxygen, experimental oxygen and inhibition of sarcoplasmic reticulum (SR) Ca^{2+} cycling on intracellular Ca^{2+} concentration ($[Ca^{2+}]_i$) in ventricular cardiomyocytes. Cardiomyocytes from juvenile turtles developed in either normoxia (21% O_2; N21) or chronic hypoxia (10% O_2, H10) were subjected to simulated normoxia (21% O_2), anoxia (0% O_2) and reoxygenation (21% O_2). A proportion of cells were treated with the inhibitors ryanodine and thapsigargin, to inhibit Ca^{2+} cycling by the SR. Control N21 and H10 cells are represented by the red and blue traces, respectively, and SR-inhibited N21 and H10 cells are represented by the black and grey traces, respectively, as described in the key.

anoxia (Fig. 2A,B), which was linked to a parallel recovery in $\Delta[Ca^{2+}]_i$ after 25 min of anoxia (Fig. 2D), despite a persistent and significant acidosis (Fig. 2H). Anoxia also significantly slowed the time to rise in both N21 and H10 cells and the time to half-decay only in H10 cells (Tables 4 and 5). Moreover, the time to half-decay was significantly slower in H10 cells, relative to N21 cells (Table 5). In line with our previous study (Ruhr et al., 2019), anoxic perfusion initially reduced shortening and $\Delta[Ca^{2+}]_i$ in N21 and H10 cells, yet these variables recovered for H10 cardiomyocytes, despite the absence of oxygen.

Reoxygenation restored shortening to pre-anoxic levels in N21 cells, in association with a recovery in $\Delta[Ca^{2+}]_i$ and a significant alkalosis (Fig. 2). Nevertheless, diastolic $[Ca^{2+}]_i$ remained significantly, although modestly, elevated in N21 and H10 cells relative to pre-anoxic levels, whereas systolic $[Ca^{2+}]_i$ was modestly, yet significantly, higher in H10 cardiomyocytes, but not in N21 cells. (Fig. 3). While the times to rise and half-decay were restored to pre-anoxic levels in H10 cells, they were significantly faster in N21 cells (Tables 4 and 5). In contrast to the normoxic period, cardiomyocyte shortening was significantly greater in H10 cells than in N21 cells after reoxygenation, but this was not linked to increased $\Delta[Ca^{2+}]_i$, which was significantly higher in N21 cells versus H10 cells (Fig. 2). At the end of the reoxygenation period, diastolic $[Ca^{2+}]_i$ was significantly higher in the N21 versus H10 cells (Fig. 3). Even though reoxygenation restored shortening and $\Delta[Ca^{2+}]_i$ in N21 and H10 cells, H10 shortening rebounded to a significantly higher level than in the N21 group.

Anoxia and reoxygenation in SR-inhibited N21 and H10 cells

The effects of simulated anoxia and reoxygenation on N21 and H10 cardiomyocyte shortening, $\Delta[Ca^{2+}]_i$ and pH_i were similar between SR-inhibited cells and control cells, but the effects were significantly more pronounced in N21 cells (Fig. 2). Shortening of N21 and H10 cardiomyocytes was significantly smaller in SR-inhibited cells during anoxia and reoxygenation across all time points, compared with that of control cells (Fig. 2A,B). The recovery in shortening of H10 cells in the latter stages of anoxia was abolished by SR inhibition, which was mirrored by significant decreases in $\Delta[Ca^{2+}]_i$ and pH_i (Fig. 2B,D,H), as well as significantly higher diastolic $[Ca^{2+}]_i$ (Fig. 3B). In N21 cells, the reduction in shortening was also associated with significant decreases in $\Delta[Ca^{2+}]_i$ and pH_i (Fig. 2A,C,G), which was driven by

Table 3. Statistical output from the generalised linear mixed-effects models

		Single factors			Interactions			Full factorial
Variable	Statistical output	Dev. O_2	Time	SR inh.	Dev. O_2×Time	Dev. O_2×SR inh.	Time×SR inh.	Dev. O_2×Time×SR inh.
Shortening	*F*-value	12.29	41.96	21.55	4.36	0.66	4.89	0.66
	P-value	**≤0.001**	**≤0.001**	**≤0.001**	**0.014**	0.419	**0.008**	0.519
$\Delta[Ca^{2+}]_i$	*F*-value	4.69	17.38	16.87	1.66	0.24	0.77	5.01
	P-value	**0.031**	**≤0.001**	**≤0.001**	0.191	0.622	0.463	**0.007**
Normalised $\Delta[Ca^{2+}]_i$	*F*-value	2.41	11.22	≤0.01	0.91	≤0.01	2.93	8.4
	P-value	0.122	**≤0.001**	0.963	0.403	0.905	0.056	**≤0.001**
pH_i	*F*-value	≤0.01	142.98	4.25	2.57	≤0.01	3.29	3.49
	P-value	0.923	**≤0.001**	**0.04**	0.078	0.998	**0.039**	**0.042**
Diastolic $[Ca^{2+}]_i$	*F*-value	4.65	29.45	0.41	4.8	0.50	0.56	1.55
	P-value	**0.032**	**≤0.001**	0.521	**0.009**	0.481	0.574	0.214
Systolic $[Ca^{2+}]_i$	*F*-value	5.85	42.54	0.16	7.14	0.29	4.60	3.18
	P-value	**0.016**	**≤0.001**	0.692	**≤0.001**	0.591	**0.011**	**0.043**
Time to rise	*F*-value	≤0.01	16.67	1.10	1.24	≤0.01	3.38	3.49
	P-value	0.91	**≤0.001**	0.296	0.29	0.905	**0.047**	**0.043**
Time to half-decay	*F*-value	2.92	6.92	33.58	0.81	0.18	5.55	0.92
	P-value	0.089	**≤0.001**	**≤0.001**	0.446	0.669	**0.004**	0.401

The fixed factors were developmental O_2 (Dev. O_2), time/experimental O_2 and inhibition of the sarcoplasmic reticulum (SR inh.). *F*- and *P*-values of the fixed factors and their interactions are presented above. Bold values indicate the effect of a single factor or an interaction between factors was significant ($P \leq 0.05$).

Journal of Experimental Biology (2024) 227, jeb247434. doi:10.1242/jeb.247434

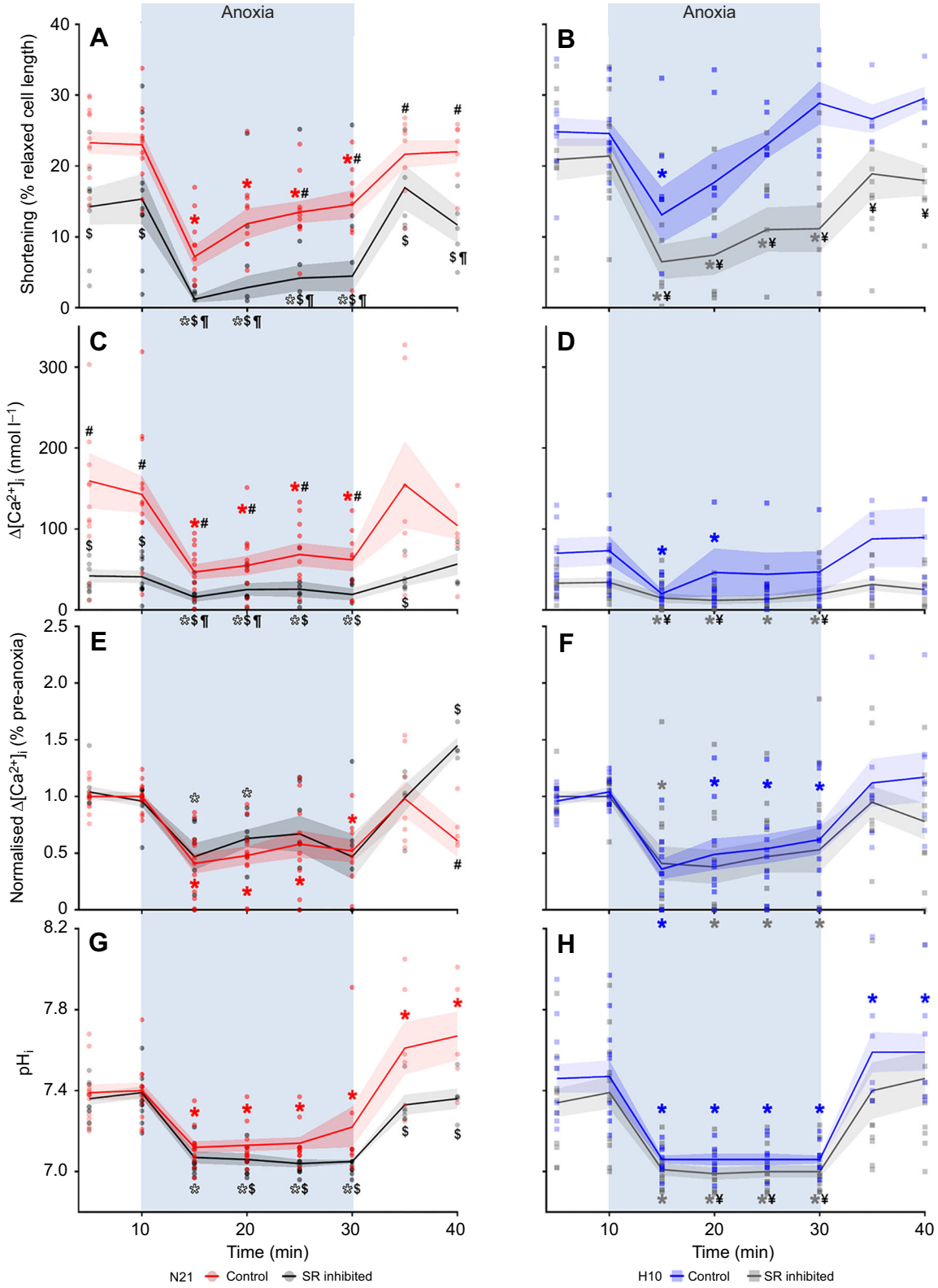

Developmental O_2-dependent effects: #, N21 control vs H10 control; ¶, N21 SR inhibited vs H10 vs SR inhibited

Experimental O_2-dependent effects (different from 5 min): ✶: red, N21 control; blue, H10 control; white, N21 SR inhibited; grey, H10 SR inhibited

Inhibitor-dependent effects: $, N21 control vs N21 SR inhibited; ¥, H10 control vs H10 SR inhibited

Fig. 2. See next page for legend.

Journal of Experimental Biology (2024) 227, jeb247434. doi:10.1242/jeb.247434

Fig. 2. Effects of anoxia and reoxygenation on shortening and ion homeostasis in ventricular cardiomyocytes. Cardiomyocytes were isolated from juvenile turtles developed in normoxia (N21; A,C,E,G) or chronic hypoxia (H10; B,D,F,H), and then subjected to simulated normoxia (21% O_2), anoxia (0% O_2) and reoxygenation (21% O_2). A subset of the cells was treated with the sarcoplasmic-reticulum (SR) inhibitors ryanodine and thapsigargin. (A,B) Cell shortening was normalised to the relaxed cell length and plotted as a percentage. (C–F) The absolute (C,D) and normalised (E,F) intracellular Ca^{2+} transient ($\Delta[Ca^{2+}]_i$). (G,H) Intracellular pH (pH_i). Values are means±s.e.m. (solid curves and shaded regions, respectively). Individual data points are plotted for each treatment group; initial *n*-values were *n*=12 N21 control, *n*=10 N21 SR inhibition, *n*=11 H10 control and *n*=12 H10 SR inhibition. When possible, cardiomyocyte shortening, $\Delta[Ca^{2+}]_i$ and pH_i were measured simultaneously. Note that some *n*-values decreased throughout the 40 min experimental period, as a result of cell death or alternans, as shown in Table S2. Statistical significance ($P \leq 0.05$) was revealed by repeated-measures, generalised linear mixed-effects models, followed by Šidák *post hoc* tests (for multiple comparisons), as indicated in the key.

higher diastolic and systolic Ca^{2+} (Fig. 3A,C). SR inhibition during anoxia also significantly hastened the time to rise in N21 cells and the time to half-decay in N21 and H10 cells (Tables 4 and 5, Fig. 1). When $\Delta[Ca^{2+}]_i$ was normalised to pre-anoxic levels, it was clear that SR inhibition in H10 and N21 cells did not change the shape of the $\Delta[Ca^{2+}]_i$ response to anoxia and reoxygenation (Fig. 2C,D), it just reduced the amount of Ca^{2+} available for contraction (Fig. 2C,D). SR inhibition had the expected effect, in that it significantly reduced shortening and $\Delta[Ca^{2+}]_i$ in N21 and H10 cells to the same levels, thus highlighting the reliance of N21 and H10 cells on SR Ca^{2+} mobilisation under anoxic conditions.

During reoxygenation, shortening, $\Delta[Ca^{2+}]_i$ and pH_i in SR-inhibited N21 and H10 cells recovered to pre-anoxic levels, but shortening and pH_i remained significantly lower than in control cells (Fig. 2). The depression in shortening was not associated with any significant differences in $\Delta[Ca^{2+}]_i$, pH_i, diastolic Ca^{2+} or systolic Ca^{2+} (Figs 2 and 3), but was linked to significant decreases in the time to half-decay in both the N21 and H10 cells, relative to control cells (Table 5). The effect of reoxygenation on SR-inhibited cells contrasted the effect on control cells, in that shortening of SR-inhibited N21 and H10 cells rebounded to the same level during

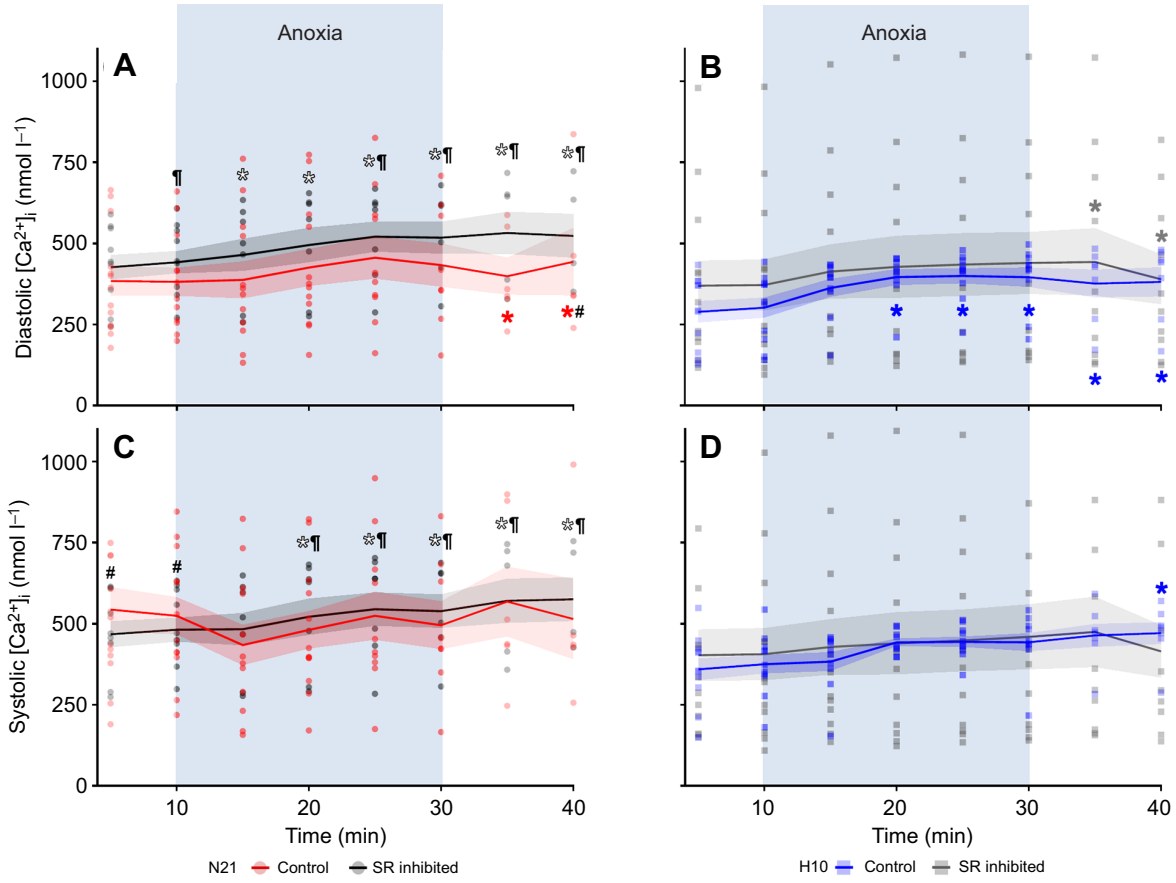

Fig. 3. Effects of anoxia and reoxygenation on diastolic and systolic $[Ca^{2+}]_i$ in ventricular cardiomyocytes. Cardiomyocytes were isolated from juvenile turtles developed in normoxia (N21; A,C) or chronic hypoxia (H10; B,D), and then subjected to simulated normoxia (21% O_2), anoxia (0% O_2) and reoxygenation (21% O_2). A subset of the cells was treated with the sarcoplasmic-reticulum (SR) inhibitors ryanodine and thapsigargin. (A,B) Diastolic and (C,D) systolic $[Ca^{2+}]_i$. Values are means±s.e.m. (solid curves and shaded regions, respectively). Individual data points are plotted for each treatment group; initial *n*-values were *n*=12 N21 control, *n*=10 N21 SR inhibition, *n*=11 H10 control and *n*=12 H10 SR inhibition. When possible, cardiomyocyte shortening, $\Delta[Ca^{2+}]_i$ and pH_i were measured simultaneously. Note that some *n*-values decreased throughout the 40 min experimental period, as a result of cell death or alternans, as shown in Table S2. Statistical significance ($P \leq 0.05$) was revealed by repeated-measures, generalised linear mixed-effects models, followed by Šidák *post hoc* tests (for multiple comparisons), as indicated in the key.

Table 4. The effect of anoxia and reoxygenation on the time to rise of the calcium transients ($\Delta[Ca^{2+}]_i$) in ventricular cardiomyocytes of juvenile turtles that embryonically developed in either normoxia (21% O_2; N21) or chronic hypoxia (10% O_2; H10)

		Time to rise (ms)		
Developmental incubation	Inhibitor treatment	Normoxia	Anoxia	Reoxygenation
N21	Control	755.5±99.5	1333.8±263.4*	367.2±114.2*
	SR inhibition	590.5±58.2	688.3±103.3$^{\$}$	532.9±130.3
H10	Control	603±93.2	1108.7±192.7*	771.3±117
	SR inhibition	664.3±126.0	1042.4±187.5	537.5±98.6

Cardiomyocytes were isolated from juvenile turtles and then subjected to simulated normoxia (21% O_2), anoxia (0% O_2) and reoxygenation (21% O_2). A subset of the cells was treated with the SR inhibitors ryanodine and thapsigargin. Values are means±s.e.m. Initial *n*-values were *n*=12 N21 control, *n*=10 N21 SR inhibition, *n*=11 H10 control and *n*=12 H10 SR inhibition. When possible, cardiomyocyte shortening, $\Delta[Ca^{2+}]_i$ and pH_i were measured simultaneously. Note that some *n*-values decreased throughout the 40 min experimental period, as a result of cell death or alternans, as shown in Table S2. Statistical significance ($P \leq 0.05$) was revealed by repeated-measures, generalised linear mixed-effects models, followed by Šidák *post hoc* tests (for multiple comparisons). Differences from the 5 min data are indicated by asterisks (*; one-tailed tests). Differences between control and SR-inhibited N21 cells are indicated by dollar signs ($^{\$}$; one-tailed tests).

reoxygenation (i.e. no significant difference between SR-inhibited N21 and H10 cells).

Cardiomyocyte myofilament Ca^{2+} sensitivity

There were significant positive regressions between shortening and $\Delta[Ca^{2+}]_i$ for control and SR-inhibited N21 cells (Fig. 4A) and for SR-inhibited H10 cells, but not control H10 cells (Fig. 4B). When controlling for $\Delta[Ca^{2+}]_i$ (i.e. using $\Delta[Ca^{2+}]_i$ as the covariate), the GLMM revealed a significant effect of developmental oxygen. That is, for a given $\Delta[Ca^{2+}]_i$ value, control or SR-inhibited H10 cells shortened significantly more than N21 cells (i.e. control H10 cells shortened more than control N21 cells and SR-inhibited H10 cells shorten more than SR-inhibited N21 cells). Additionally, there was a significant effect of SR inhibition; for a given $\Delta[Ca^{2+}]_i$ value, control N21 or H10 cells shortened significantly more than their SR-inhibited counterparts (i.e. control N21 cells shorten more than SR-inhibited N21 cells and control H10 cells shorten more than SR-inhibited H10 cells). See Table S3 for full details of these statistical interactions.

An effect of pH_i on shortening was also observed. There were significant positive regressions between shortening and pH_i in control and SR-inhibited N21 cells, but not in H10 cells (Fig. S2). When controlling for pH_i, the GLMM revealed no significant effect of developmental oxygen (i.e. pH_i affected N21 and H10 control cells and N21 and H10 SR-inhibited cells similarly), but demonstrated a significant effect of SR inhibition. Namely, for a given pH_i value, control N21 or H10 cells shortened significantly more than their SR-inhibited counterparts (i.e. control N21 cells shorten more than SR-inhibited N21 cells and control H10 cells shorten more than SR-inhibited H10 cells). See Table S3 for full details of these statistical interactions.

These analyses demonstrate that shortening in H10 cardiomyocytes is more sensitive to $[Ca^{2+}]_i$, leading to greater shortening by H10 versus N21 cells for the same $\Delta[Ca^{2+}]_i$ value, which is abolished by SR inhibition. The effect of pH_i on cardiomyocyte shortening is also clear; control H10 shortening is unaffected by changes in pH_i, when SR Ca^{2+} stores are available, unlike SR-inhibited H10 shortening.

DISCUSSION

The developing vertebrate heart is capable of extraordinary phenotypic plasticity in response to oxygen deprivation. Although the extent of cardiac remodelling depends on embryonic stage (Burggren and Mueller, 2015), chronic developmental hypoxia consistently changes cardiovascular function in all vertebrate classes [e.g. mammals (Peyronnet et al., 2002), birds (Villamor et al., 2004), reptiles (Crossley et al., 2022), amphibians (Pan and Burggren, 2013) and fish (Robertson et al., 2014)], as well as invertebrates [e.g. crustaceans (Gopel and Burggren, 2024)]. Nevertheless, only a handful of studies have characterised the cellular and molecular mechanisms that underpin the phenotypes of hypoxia-programmed hearts in ectotherms. The SR of the ectothermic vertebrate heart is a structure that can be modified, providing a source of phenotypic flexibility to elevate heart performance, when faced with an environmental stressor (Shiels and Galli, 2014).

In the present study, we found that chronic developmental hypoxia reduced turtle cardiomyocyte reliance on SR Ca^{2+} cycling under normoxic conditions and increased the sensitivity of the myofilaments to Ca^{2+}. We also show that, regardless of

Table 5. The effect of anoxia and reoxygenation on the time to half-decay of the calcium transient ($\Delta[Ca^{2+}]_i$) in ventricular cardiomyocytes of juvenile turtles that embryonically developed in either normoxia (21% O_2; N21) or chronic hypoxia (10% O_2; H10)

		Time to half-decay (ms)		
Developmental incubation	Inhibitor treatment	Normoxia	Anoxia	Reoxygenation
N21	Control	742.5±89.0	534.5±158.1$^{*,\#}$	533.2±172.9*
	SR inhibition	344.2±69.1$^{\$}$	239.7±61.1$^{\$}$	181.7±42.8$^{\$}$
H10	Control	717.9±118.3	1060.8±128.2*	800.8±152.1
	SR inhibition	447.3±125.7$^{¥}$	429.6±139.2$^{¥}$	229.4±82.2$^{¥}$

Cardiomyocytes were isolated from juvenile turtles and then subjected to simulated normoxia (21% O_2), anoxia (0% O_2) and reoxygenation (21% O_2). A subset of the cells was treated with the SR inhibitors ryanodine and thapsigargin. Values are means±s.e.m. Initial *n*-values were *n*=12 N21 control, *n*=10 N21 SR inhibition, *n*=11 H10 control and *n*=12 H10 SR inhibition. When possible, cardiomyocyte shortening, $\Delta[Ca^{2+}]_i$ and pH_i were measured simultaneously. Note that some *n*-values decreased throughout the 40 min experimental period, as a result of cell death or alternans, as shown in Table S2. Statistical significance ($P \leq 0.05$) was revealed by repeated-measures, generalised linear mixed-effects models, followed by Šidák *post hoc* tests (for multiple comparisons). Differences between control N21 and H10 cells are indicated by hash symbols ($^{\#}$; two-tailed tests). Differences from the 5 min data are indicated by asterisks (*; one-tailed tests). Differences between control and SR-inhibited N21 cells are indicated by dollar signs ($^{\$}$) and between control and SR-inhibited H10 cells by yen signs ($^{¥}$; one-tailed tests).

Journal of Experimental Biology (2024) 227, jeb247434. doi:10.1242/jeb.247434

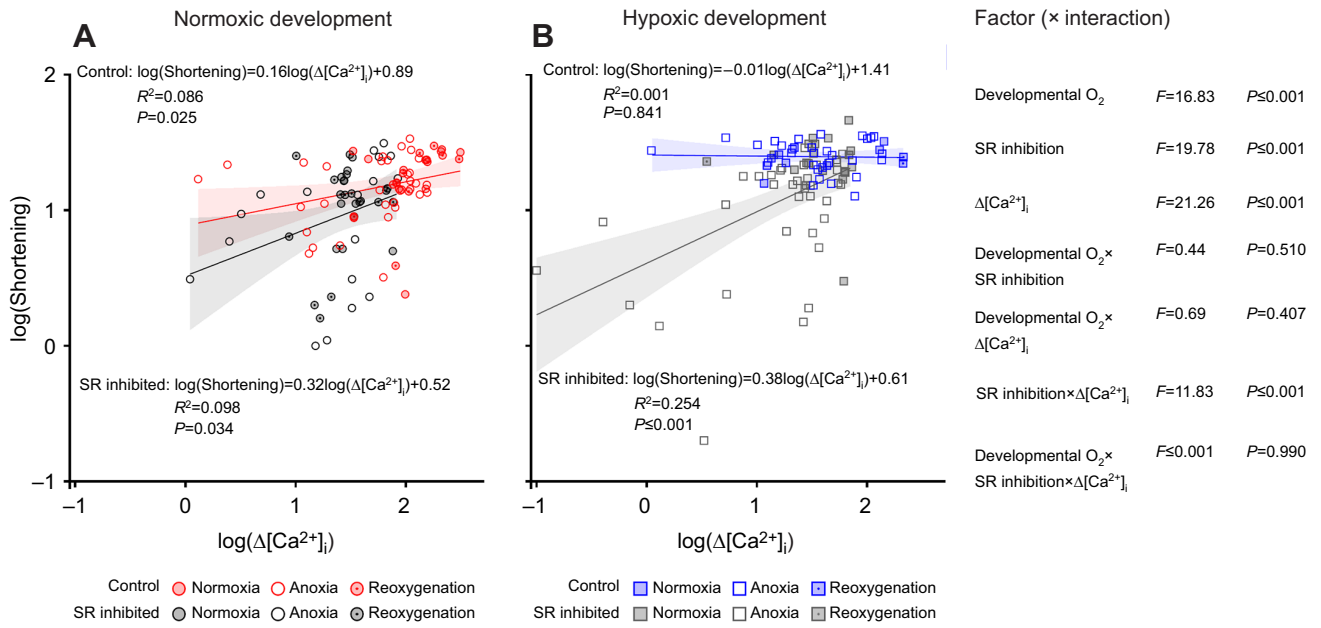

Fig. 4. The effects of developmental hypoxia and inhibited SR Ca^{2+} cycling on myofilament Ca^{2+} sensitivity. Cardiomyocytes were isolated from juvenile turtles developed in normoxia (N21; A) or chronic hypoxia (H10; B), and then subjected to simulated normoxia (21% O_2), anoxia (0% O_2) and reoxygenation (21% O_2). A subset of the cells was treated with the sarcoplasmic-reticulum (SR) inhibitors ryanodine and thapsigargin. The regression lines (±95% confidence intervals) show the relationship between shortening and $\Delta[Ca^{2+}]_i$ in N21 and H10 cardiomyocytes. Data from normoxia, anoxia and reoxygenation treatments were pooled to produce the regressions, so that the effect of developmental environment and SR inhibition could be emphasised. Shortening was the dependent variable, developmental oxygen and SR inhibition were the fixed factors, and $\Delta[Ca^{2+}]_i$ was the covariate. Regressions were considered significant when $P \leq 0.05$. The results of the generalised linear mixed-effects model are presented to the right of B (only main effects are displayed; results from the multiple-comparison analyses are presented in Table S3). Control and SR-inhibited N21 cells are represented by circles, whereas control and SR-inhibited H10 cells are represented by squares, as described in the key.

developmental oxygen levels, cardiomyocyte shortening during anoxia and reoxygenation is dependent on SR Ca^{2+} cycling. However, hypoxic development increased the reliance on the SR, given that anoxic recovery of shortening and intracellular calcium transients ($\Delta[Ca^{2+}]_i$) in the H10 cells is abolished by SR inhibition. These results collectively suggest that chronic developmental hypoxia programmes SR function; specifically, it alters intracellular Ca^{2+} cycling in the ventricular cardiomyocytes of juvenile snapping turtles, which has implications for contractility in normoxia and during anoxia/reoxygenation. Accordingly, we demonstrate that freshwater turtles are dependent on the SR when the heart is challenged by anoxia.

Developmental hypoxia alters cardiomyocyte physiology under normoxic conditions

Developmental hypoxia has a potent effect on the snapping-turtle heart. It causes relative cardiac enlargement in embryos (Tate et al., 2015) and, in agreement with prior studies (Galli et al., 2021; Ruhr et al., 2021), we show that this phenotype persists into juvenile life (Table 2). Despite the cardiac enlargement, developmental hypoxia decreased the length of snapping turtle ventricular cardiomyocytes (Table 2), which is coupled to alterations in cellular function, a result we have previously shown (Ruhr et al., 2019). The most notable observation from the present and previous studies (Ruhr et al., 2019) is that H10 cardiomyocytes produce remarkably smaller $\Delta[Ca^{2+}]_i$ than N21 cells in normoxia, without affecting shortening (Fig. 2A–D). Here, we show that SR inhibition reduced N21 $\Delta[Ca^{2+}]_i$ to H10 levels, and this was associated with a reduction in systolic Ca^{2+}. These findings suggest that developmental hypoxia reduces ventricular cardiomyocyte reliance on SR Ca^{2+} cycling, leading to smaller $\Delta[Ca^{2+}]_i$. Despite the lower $\Delta[Ca^{2+}]_i$, H10 shortening was similar to that of N21 cells in normoxia, and we previously showed this is driven by enhanced myofilament Ca^{2+} sensitivity (Ruhr et al., 2019) that is likely epigenetically programmed by hypoxia during embryogenesis, which we discuss below (Ruhr et al., 2021).

A hallmark of ventricular myofibrils in ectothermic vertebrates is high Ca^{2+} sensitivity, relative to endotherms, and modulation of Ca^{2+} sensitivity commonly occurs to maintain contractility in response to acute or chronic changes in oxygen, pH, temperature and phosphate (Churcott et al., 1994; Fanter et al., 2017; Klaiman et al., 2014; Ruhr et al., 2019). These studies suggest that an environmental stressor, such as developmental hypoxia, might reorganise EC-coupling pathways in turtle cardiomyocytes, which acts to reduce SR Ca^{2+} reliance and increase myofilament Ca^{2+} sensitivity. This notion is supported by studies on fetal sheep subjected to chronic, high-altitude hypoxia, which alters the abundance of RyRs, lowers activator Ca^{2+} availability and increases myofilament Ca^{2+} sensitivity (Browne et al., 1997; Onishi et al., 2004). Developmental hypoxia could likewise modify EC coupling in snapping turtles, leading to similar shortening of N21 and H10 cardiomyocytes under normoxic conditions, but achieved through different mechanisms.

Plasticity of SR morphology and function has been demonstrated in numerous adult ectothermic vertebrates that are exposed to chronic stress. For instance, mobilisation of SR Ca^{2+} increases contractility at cold temperature in the highly active bluefin tuna (*Thunnus thynnus*), bigeye tuna (*Thunnus obesus*), mahi-mahi (*Coryphaena hippurus*) and swordfish (*Xiphias gladius*) (Galli et al., 2009a; Shiels et al., 2011). Furthermore, SR Ca^{2+} becomes important for maintaining force production in rainbow trout and Alaskan blackfish, when they are acutely or chronically warmed (Kubly and Stecyk, 2019; Shiels and Farrell, 1997). More pertinent

to our results is the reliance on SR Ca^{2+} cycling that is required to tolerate anoxia in the heart of the Amazonian armoured catfish (MacCormack et al., 2003). As with the snapping turtle, inhibition of the SR, during anoxia, substantially reduced heart function in the catfish. Taken together, these earlier studies demonstrate the cardioprotective role the SR plays in the hearts of stress-challenged ectotherms.

The cellular and molecular mechanisms that drive reduced SR Ca^{2+} cycling and enhanced myofilament Ca^{2+} sensitivity in H10 cells are largely unknown, but might involve epigenetic regulation. Myofilament Ca^{2+} sensitivity is susceptible to perturbations in the developmental environment, and developmental programming can modulate the expression of proteins associated with myofilament–Ca^{2+} binding affinity. For example, gene expression patterns of cardiac troponin are modified by DNA methylation in embryonic mice (Xu et al., 2015). Likewise, we have shown developmental hypoxia differentially methylates and enhances the expression of genes encoding cardiac-type troponin T2 (*tnnt2*), tropomyosin 3 (*tpm3*) and myosin-light chain 1 (*myl1*) in juvenile snapping turtles (Ruhr et al., 2021). Mutations in these genes change the sensitivity of the myofilaments to Ca^{2+} in mammalian systems, but through distinct mechanisms (Marston, 2018). Because these proteins modulate Ca^{2+}-dependent myofilament contractility, their elevated synthesis could enhance myofibril Ca^{2+} sensitisation in turtles (Fig. 4), as it does in mammals. Moreover, developmental hypoxia upregulates the genes *bmp10* (ligand) and *bmpr2* (BMP10 receptor) in snapping turtle hearts (Ruhr et al., 2021), which are linked to healthy contractile function in mice (Umbarkar et al., 2019). When rat BMPR2 is not synthesised, it impairs cardiac myofilament–Ca^{2+} binding and decreases contractility (Hautefort et al., 2019).

We can only speculate on the mechanism driving the reduced reliance on SR Ca^{2+} cycling in H10 cardiomyocytes. It is possible that developmental hypoxia alters the gene expression of SR proteins via epigenetic regulation, such as DNA methylation. A reduction in RyR protein abundance would explain the lower levels of systolic Ca^{2+} in H10 versus N21 cardiomyocytes, whereas a reduction in SERCA protein abundance could reduce SR Ca^{2+} content and slow the $\Delta[Ca^{2+}]_i$ decay. While we did not find differences in the methylation patterns of genes encoding SR proteins, we did find differences in genes that are known to regulate SR function. For instance, the promoter regions of *ryr3* (RyR) and *atp2a3* (SERCA) are differentially methylated by developmental hypoxia in the snapping turtle heart (Ruhr et al., 2021). Methylation of these genes' promoter regions reduces their RNA expression and protein abundance in the mammalian heart and brain (Kao et al., 2010; Mackrill, 2010; Rabkin and Wong, 2023; Torres and Kerr, 2021). Furthermore, we found that cardiac genes encoding the transcription factors hypoxia-inducible factor 1 (*hif1A*) and nuclear-factor kappa beta (*nfkβ*) were upregulated in H10 turtles (Ruhr et al., 2021). In mammals, higher protein abundance of HIF1A and NFKβ suppresses SERCA protein synthesis (Ronkainen et al., 2011; Tsai et al., 2015; Williams et al., 2019). Alternatively, reliance on SR Ca^{2+} cycling could be reduced by an overall reduction in cardiac SR density or a reorganisation of SR–couplon activity, which occurs in response to either chronic oxygen deprivation or metabolic inhibition in mammals (Chantawansri et al., 2008; Guski et al., 1981; Schaper et al., 1977). Lastly, developmental hypoxia might alter SR Ca^{2+} cycling via post-translational modifications, such as oxidation of RyR and calmodulin (Oda et al., 2015).

In contrast to our findings in snapping turtles, our previous work on red-eared sliders suggests cardiomyocyte contractility is entirely dependent on trans-sarcolemmal Ca^{2+} cycling in normoxia, without any contribution from the SR (Galli et al., 2006a,b). It is thought that SR Ca^{2+} cycling is more common in active species of ectotherms (Galli et al., 2009a,b, 2006a; Keen et al., 1992; Shiels et al., 2011, 1999; Shiels and Farrell, 2000), since they require higher levels of cardiac output. In this scenario, the SR provides an additional source of Ca^{2+} that can be released during systole, leading to higher force generation. Considering that North American freshwater turtles are relatively sedentary reptiles and that common snapping turtles and slider turtles share similar ecological niches and life histories (Ultsch, 2006), it is surprising to discover that snapping turtle cardiomyocytes use SR Ca^{2+} stores for contraction and relaxation, unlike slider turtles. However, this result is consistent with earlier findings that ventricular force production in isolated muscle strips is roughly twofold higher in snapping turtles than in slider turtles (Galli et al., 2006a; Smith et al., 2022). The reason for the difference in SR reliance between snapping and slider turtles remains to be investigated, but it might be related to several factors, including laboratory conditions (e.g. age, sex, developmental conditions, husbandry, etc.) or wild behaviours (e.g. foraging, diet, daily movements/migrations, etc.). Nevertheless, previous measures of cardiovascular function are comparable between the two species (e.g., heart rate, stroke volume, cardiac output, ventricular pressure) (Galli et al., 2004; Gatten, 1988; Overgaard et al., 2002; Ruhr et al., 2021; Smith et al., 2022; Stecyk and Farrell, 2007). Therefore, it would be interesting to see whether this is also the case during some form of exercise, such as foraging.

Effects of simulated anoxia on cardiomyocyte function

Acute anoxia severely impaired shortening in N21 and H10 cardiomyocytes, which is consistent with *in vivo* and *in vitro* studies on snapping turtles (Ruhr et al., 2021; Ruhr et al., 2019), painted turtles [*Chrysemys picta* (Jackson, 1987)] and slider turtles (Stecyk et al., 2009). As in our previous study (Ruhr et al., 2019), the anoxia-induced reduction in shortening was due to a combination of reduced $\Delta[Ca^{2+}]_i$ and a profound intracellular acidosis (Fig. 2). Here, we show that the effects of anoxia were comparable between SR-inhibited N21 and H10 cells, but significantly more pronounced than in control N21 and H10 cells. The lower levels of shortening in SR-inhibited cells during anoxia was driven by a reduction in $\Delta[Ca^{2+}]_i$ that was caused by increased diastolic $[Ca^{2+}]_i$. SR inhibition also exacerbated the intracellular acidosis during anoxia (Fig. 2G,H), which is known to decrease $\Delta[Ca^{2+}]_i$ by reducing myofilament–Ca^{2+} binding affinity (Orchard and Kentish, 1990). While we did not investigate the mechanism, the lower pH_i of SR-inhibited cells could be driven by the blockade of SERCA-mediated Ca^{2+} uptake, which would potentiate Ca^{2+} efflux and Na^+ influx via NCX, leading to more Na^+ being exchanged for protons via the Na^+/H^+-exchanger (compared with control cells). Collectively, these results suggest N21 and H10 cardiomyocytes recruit SR Ca^{2+} during anoxia to maintain contractile function.

In line with our previous study (Ruhr et al., 2019), H10 shortening and $\Delta[Ca^{2+}]_i$ recovered to pre-anoxic levels at the latter stages of anoxia, while N21 shortening remained depressed throughout the anoxic challenge. We previously showed that the recovery of H10 force is partly due to a Ca^{2+}-dependent mechanism (increased myofilament Ca^{2+} sensitivity) and a Ca^{2+}-independent mechanism (a superior ability to supress ROS) during anoxia (Ruhr et al., 2019). Here, we show that the recovery is also dependent on the SR, because SR inhibition of anoxic H10 cells prevents a rebound in shortening.

Our results are consistent with other studies that show embryonic and juvenile American alligators (*Alligator mississippiensis*) and

snapping turtles exposed to developmental hypoxia have attenuated responses to an acute hypoxic challenge, with blunted responses to heart rate and blood pressure (Crossley and Altimiras, 2005; Crossley et al., 2017, 2022, 2023; Eme et al., 2011; Kam, 1993; Smith et al., 2019). Developmental programming of stress-tolerant phenotypes has also been observed in other ectothermic vertebrates and can occur by either direct (embryonic) or indirect (parental) exposure to environmental stressors. For example, exposing embryonic zebrafish (*Danio rerio*) to hypoxia lowers their critical oxygen tension (Robertson et al., 2014) and boosts metabolic plasticity (Barrionuevo et al., 2010) at the larval stage, and parental exposure to hypoxia or thermal stress results in offspring with superior hypoxia or thermal tolerance, respectively (Ho and Burggren, 2012; Massey and Dalziel, 2023). Similarly, common killifish (*Fundulus heteroclitus*) and white suckerfish (*Catostomus commersonii*) living in chronically polluted waters produce offspring with improved resistance to the pollutants (Bozinovic et al., 2022; Meyer et al., 2003; Munkittrick and Dixon, 1988). Of course, it should be noted that environmental stressors can also lead to maladaptive programming in ectothermic and endothermic vertebrates (Galli et al., 2023; Itani et al., 2018; Wu, 2009), but our results support the growing body of evidence that early exposure to hypoxia can prime the physiology of some ectotherms to better tolerate oxygen-deprived environments in later life.

Effects of simulated reoxygenation on cardiomyocyte function

Although anoxia can initiate catastrophic cell-death cascades in mammals (Bundgaard et al., 2020), reoxygenation is arguably one of the gravest threats to cellular survival, as this causes a surge in ROS production that can trigger the activation of apoptotic pathways (Murphy and Steenbergen, 2008). The mammalian response to reoxygenation stands in stark contrast to that of turtles, which do not suffer any overt cardiac dysfunction (Bundgaard et al., 2018; Galli et al., 2021; Ruhr et al., 2021, 2019; Wasser et al., 1997, 1992). Indeed, upon reoxygenation, all variables in this study returned to pre-anoxic levels in control N21 and H10 cardiomyocytes, apart from pH_i, which rebounded beyond control levels (i.e. a relative alkalosis). SR inhibition did not affect the bimodal responses to reoxygenation in N21 and H10 cardiomyocytes, but did reduce the amount of shortening relative to control cells. This suggests that SR Ca^{2+} cycling also plays a role in maintaining contractility during reoxygenation. Similar to the results during the pre-anoxic period, H10 cardiomyocytes were able to maintain shortening during reoxygenation at higher levels than N21 cardiomyocytes, despite similar levels of $\Delta[Ca^{2+}]_i$ and pH_i. While increased myofilament Ca^{2+} sensitivity undoubtedly plays a role, other factors might contribute to greater shortening of H10 cardiomyocytes during reoxygenation, such as ROS management. Excessive ROS production can impede cardiac force production, by damaging sarcomere proteins and lowering myofilament Ca^{2+} sensitivity (Sumandea and Steinberg, 2011). Compared with N21 turtles, snapping turtles from hypoxic incubations possess a superior ability to suppress cardiac ROS production (Galli et al., 2021), including the mitigation of oxidative damage to the heart. Indeed, exposure to developmental hypoxia leads to upregulation of the gene encoding peptidylprolyl isomerase A (Ruhr et al., 2021), which is an enzyme that cells produce in response to oxidative stress to suppress mitochondrial ROS production (Satoh et al., 2011). Consequently, turtles from hypoxic incubations might better protect EC-coupling components during reoxygenation, such as the SR and myofibrils. Moreover, better management of mitochondrial Ca^{2+} could help maintain contractile function and avoid triggering apoptotic pathways, such as the mitochondrial permeability transition pore (Morciano et al., 2017). Nevertheless, our results suggest that the turtle heart, irrespective of developmental oxygen levels, can withstand reoxygenation without damaging cellular function and ion homeostasis, if it exploits SR Ca^{2+}.

Perspectives

North American freshwater turtles possess the exceptional ability to survive in the complete absence of oxygen for periods lasting several months (Jackson, 2000). We have provided evidence that this anoxia-tolerant phenotype is improved in the heart by early exposure to chronic embryonic hypoxia. On a mechanistic level, our results build on our previous work to demonstrate that the hearts of snapping turtles from hypoxic incubations are less reliant on SR Ca^{2+} stores to contract under normoxic conditions, but recruit them during acute anoxia. Together, SR Ca^{2+} cycling and higher myofilament Ca^{2+} sensitivity work in concert to sustain routine levels of contractile function during anoxia and reoxygenation. These findings represent the first examples of developmental plasticity of SR function and are noteworthy, because the SR is a vital source of activator Ca^{2+} for contraction and is an essential Ca^{2+} sink during relaxation. Therefore, developmental programming of this structure has important implications for EC coupling in the vertebrate heart. From a broader ecological perspective, snapping turtles likely rely on the SR to protect cardiac function during anoxia, which allows them to thrive in their natural habitats.

Acknowledgements

We thank the staff of the Biological Services Facility, at the University of Manchester (UoM), for their help with turtle husbandry. We thank Prof Andrew Trafford (UoM) for experimental advice and Peter Ceuppens (UoM) with our statistical analyses.

Competing interests

The authors declare no competing or financial interests.

Author contributions

Conceptualization: I.M.R., G.L.J.G.; Methodology: I.M.R., H.A.S., D.A.C., G.L.J.G.; Software: I.M.R.; Validation: I.M.R., G.L.J.G.; Formal analysis: I.M.R., G.L.J.G.; Investigation: I.M.R.; Resources: H.A.S., D.A.C., G.L.J.G.; Data curation: I.M.R.; Writing - original draft: I.M.R.; Writing - review & editing: I.M.R., H.A.S., D.A.C., G.L.J.G.; Visualization: I.M.R.; Supervision: G.L.J.G.; Project administration: I.M.R., G.L.J.G.; Funding acquisition: G.L.J.G.

Funding

This study was funded by a New Investigator Grant awarded to G.L.J.G. by the Biotechnology and Biological Sciences Research Council (BBSRC grant no. BB/N005740/1). Open Access funding provided by Biotechnology and Biological Sciences Research Council. Deposited in PMC for immediate release.

Data availability

All relevant data can be found within the article and its supplementary information.

Special Issue

This article is part of the Special Issue 'The integrative biology of the heart', guest edited by William Joyce and Holly Shiels. See related articles at https://journals.biologists.com/jeb/issue/227/20.

References

Ackerman, R. A. and Lott, D. B. (2004). Thermal, hydric, and respiratory climate of nests. In *Reptilian Incubation: Environment, Evolution, and Behaviour* (ed. D. C. Deeming), pp. 15-43. Nottingham, UK: Nottingham University Press.

Alvine, T., Rhen, T. and Crossley, D. A., II. (2013). Temperature-dependent sex determination modulates cardiovascular maturation in embryonic snapping turtles, *Chelydra serpentina*. *J. Exp. Biol.* **216** , 751-758. doi:10.1242/jeb.074609

Barrionuevo, W. R., Fernandes, M. N. and Rocha, O. (2010). Aerobic and anaerobic metabolism for the zebrafish, *Danio rerio*, reared under normoxic and hypoxic conditions and exposed to acute hypoxia during development. *Braz. J. Biol.* **70**, 425-434. doi:10.1590/S1519-69842010000200027

Bateson, P., Gluckman, P. and Hanson, M. (2014). The biology of developmental plasticity and the Predictive Adaptive Response hypothesis. *J. Physiol.* **592**, 2357-2368. doi:10.1113/jphysiol.2014.271460

Bers, D. M. (2002). Cardiac excitation-contraction coupling. *Nature* **415**, 198-205. doi:10.1038/415198a

Bolker, B. M. (2015). Linear and generalized linear mixed models. In *Ecological Statistics: Contemporary Theory and Application* (ed. G. A. Fox, S. Negrete-Yankelevich and V. J. Sosa), pp. 309-333. Oxford University Press.

Booth, D. T. (2000). The effect of hypoxia on oxygen consumption of embryonic estuarine crocodiles (*Crocodylus porosus*). *J. Herpetol.* **34**, 478-481. doi:10.2307/1565377

Bossen, E. H. and Sommer, J. R. (1984). Comparative stereology of the lizard and frog myocardium. *Tissue Cell* **16**, 173-178. doi:10.1016/0040-8166(84)90042-9

Bozinovic, G., Feng, Z., Shea, D. and Oleksiak, M. F. (2022). Cardiac physiology and metabolic gene expression during late organogenesis among *F. heteroclitus* embryo families from crosses between pollution-sensitive and -resistant parents. *BMC Ecol. Evol.* **22**, 3. doi:10.1186/s12862-022-01959-1

Browne, V. A., Stiffel, V. M., Pearce, W. J., Longo, L. D. and Gilbert, R. D. (1997). Activator calcium and myocardial contractility in fetal sheep exposed to long-term, high-altitude hypoxia. *Am. J. Physiol.* **272**, H1196-H1204.

Bundgaard, A., James, A. M., Joyce, W., Murphy, M. P. and Fago, A. (2018). Suppression of reactive oxygen species generation in heart mitochondria from anoxic turtles: the role of complex I S-nitrosation. *J. Exp. Biol.* **221**, jeb174391. doi:10.1242/jeb.174391

Bundgaard, A., Ruhr, I. M., Fago, A. and Galli, G. L. J. (2020). Metabolic adaptations to anoxia and reoxygenation: New lessons from freshwater turtles and crucian carp. *Curr. Opin. Metab. Endocrin. Res.* **11**, 55-64. doi:10.1016/j.coemr.2020.01.002

Burggren, W. W. and Mueller, C. A. (2015). Developmental critical windows and sensitive periods as three-dimensional constructs in time and space. *Physiol. Biochem. Zool.* **88**, 91-102. doi:10.1086/679906

Burggren, W. W. and Reyna, K. S. (2011). Developmental trajectories, critical windows, and phenotypic alteration during cardio-respiratory development. *Respir. Physiol. Neurobiol.* **178**, 13-21. doi:10.1016/j.resp.2011.05.001

Chantawansri, C., Huynh, N., Yamanaka, J., Garfinkel, A., Lamp, S. T., Inoue, M., Bridge, J. H. and Goldhaber, J. I. (2008). Effect of metabolic inhibition on couplon behavior in rabbit ventricular myocytes. *Biophys. J.* **94**, 1656-1666. doi:10.1529/biophysj.107.114892

Chung, J. H., Biesiadecki, B. J., Ziolo, M. T., Davis, J. P. and Janssen, P. M. (2016). Myofilament calcium sensitivity: role in regulation of *in-vivo* cardiac contraction and relaxation. *Front. Physiol.* **7**, 562.

Churcott, C. S., Moyes, C. D., Bressler, B. H., Baldwin, K. M. and Tibbits, G. F. (1994). Temperature and pH effects on Ca^{2+} sensitivity of cardiac myofibrils: a comparison of trout with mammals. *Am. J. Physiol. Regul. Integr. Comp. Physiol.* **267**, R62-R70. doi:10.1152/ajpregu.1994.267.1.R62

Cros, C., Salle, L., Warren, D. E., Shiels, H. A. and Brette, F. (2014). The calcium stored in the sarcoplasmic reticulum acts as a safety mechanism in rainbow trout heart. *Am. J. Physiol. Regul. Integr. Comp. Physiol.* **307**, R1493-R1501. doi:10.1152/ajpregu.00127.2014

Crossley, D. A., , II and Altimiras, J. (2005). Cardiovascular development in embryos of the American alligator, *Alligator mississippiensis*: effects of chronic and acute hypoxia. *J. Exp. Biol.* **208** , 31-39. doi:10.1242/jeb.01355

Crossley, D. A., , II, Ling, R., Nelson, D., Gillium, T., Conner, J., Hapgood, J., Elsey, R. M. and Eme, J. (2017). Metabolic responses to chronic hypoxic incubation in embryonic American alligators (*Alligator mississippiensis*). *Comp. Biochem. Physiol. A Mol. Integr. Physiol.* **203**, 77-82. doi:10.1016/j.cbpa.2016.08.017

Crossley, J. L., Lawrence, T., Tull, M., Elsey, R. M., Wang, T. and Crossley, D. A., II. (2022). Developmental oxygen preadapts ventricular function of juvenile American alligators, *Alligator mississippiensis*. *Am. J. Physiol. Regul. Integr. Comp. Physiol.* **323**, R739-R748. doi:10.1152/ajpregu.00059.2022

Crossley, J. L., Smith, B., Tull, M., Elsey, R. M., Wang, T. and Crossley, D. A., II. (2023). Hypoxic incubation at 50% of atmospheric levels shifts the cardiovascular response to acute hypoxia in American alligators, *Alligator mississippiensis*. *J. Comp. Physiol. B* **193**, 545-556. doi:10.1007/s00360-023-01510-8

Eme, J., Hicks, J. W. and Crossley, D. A., II. (2011). Chronic hypoxic incubation blunts a cardiovascular reflex loop in embryonic American alligator (*Alligator mississippiensis*). *J. Comp. Physiol. B* **181**, 981-990. doi:10.1007/s00360-011-0569-z

Eme, J., Rhen, T. and Crossley, D. A., II. (2014). Adjustments in cholinergic, adrenergic, and purinergic control of cardiovascular function in snapping turtle embryos (*Chelydra serpentina*) incubated in chronic hypoxia. *J. Comp. Physiol. B* **184**, 891-902. doi:10.1007/s00360-014-0848-6

Eme, J., Rhen, T., Tate, K. B., Gruchalla, K., Kohl, Z. F., Slay, C. E. and Crossley, D. A., II. (2013). Plasticity of cardiovascular function in snapping turtle embryos (*Chelydra serpentina*): chronic hypoxia alters autonomic regulation and gene expression. *Am. J. Physiol. Regul. Integr. Comp. Physiol.* **304**, R966-R979. doi:10.1152/ajpregu.00595.2012

Eme, J., Tate, K. B., Rhen, T. and Crossley, D. A., II. (2021). Cardiovascular responses to putative chemoreceptor stimulation of embryonic common snapping turtles (*Chelydra serpentina*) chronically incubated in hypoxia (10% O_2). *Comp. Biochem. Physiol. A Mol. Integr. Physiol.* **259**, 110977. doi:10.1016/j.cbpa.2021.110977

Fanter, C. E., Campbell, K. S. and Warren, D. E. (2017). The effects of pH and P_i on tension and Ca^{2+} sensitivity of ventricular myofilaments from the anoxia-tolerant painted turtle. *J. Exp. Biol.* **220**, 4234-4241. doi:10.1242/jeb.164137

Frische, S., Fago, A. and Altimiras, J. (2000). Respiratory responses to short-term hypoxia in the snapping turtle, *Chelydra serpentina*. *Comp. Biochem. Physiol. A Mol. Integr. Physiol.* **126**, 223-231. doi:10.1016/S1095-6433(00)00201-4

Galli, G. L. J., Taylor, E. W. and Wang, T. (2004). The cardiovascular responses of the freshwater turtle, *Trachemys scripta*, to warming and cooling. *J. Exp. Biol.* **207**, 1471-1478. doi:10.1242/jeb.00912

Galli, G. L., Shiels, H. A. and Brill, R. W. (2009a). Temperature sensitivity of cardiac function in pelagic fishes with different vertical mobilities: yellowfin tuna (*Thunnus albacares*), bigeye tuna (*Thunnus obesus*), mahimahi (*Coryphaena hippurus*), and swordfish (*Xiphias gladius*). *Physiol. Biochem. Zool.* **82**, 280-290. doi:10.1086/597484

Galli, G. L. J., Warren, D. E. and Shiels, H. A. (2009b). Ca^{2+} cycling in cardiomyocytes from a high-performance reptile, the varanid lizard (*Varanus exanthematicus*). *Am. J. Physiol. Regul. Integr. Comp. Physiol.* **297**, R1636-R1644. doi:10.1152/ajpregu.00381.2009

Galli, G. L. J., Gesser, H., Taylor, E. W., Shiels, H. A. and Wang, T. (2006a). The role of the sarcoplasmic reticulum in the generation of high heart rates and blood pressures in reptiles. *J. Exp. Biol.* **209**, 1956-1963. doi:10.1242/jeb.02228

Galli, G. L. J., Taylor, E. W. and Shiels, H. A. (2006b). Calcium flux in turtle ventricular myocytes. *Am. J. Physiol. Regul. Integr. Comp. Physiol.* **291**, R1781-R1789. doi:10.1152/ajpregu.00421.2006

Galli, G. L. J., Ruhr, I. M., Crossley, J. and Crossley, D. A., II. (2021). The long-term effects of developmental hypoxia on cardiac mitochondrial function in snapping turtles. *Front. Physiol.* **12**, 689684. doi:10.3389/fphys.2021.689684

Galli, G. L. J., Lock, M. C., Smith, K. L. M., Giussani, D. A. and Crossley, D. A., II. (2023). Effects of developmental hypoxia on the vertebrate cardiovascular system. *Physiology* **38**, 0.

Gatten, R. E., Jr. (1980). Aerial and aquatic oxygen uptake by freely-diving snapping turtles (*Chelydra serpentina*). *Oecologia* **46**, 266-271. doi:10.1007/BF00540136

Gatten, R. E., Jr. (1988). Cardiovascular correlates of exercise in snapping turtles, *Chelydra serpentina*. *Comp. Biochem. Physiol. A Comp. Physiol.* **90**, 53-56. doi:10.1016/0300-9629(88)91004-3

Gillis, T. E. (2011). Cardiac excitation-contraction coupling: Calcium and the contractile element. In *Encyclopedia of Fish Physiology: From Genome to Environment*, Vol. 2 (ed. A. P. Farrell, E. D. Stevens, J. Cech and J. G. Richards), pp. 1054-1059. Academic Press.

Giussani, D. A. (2021). Breath of life: Heart-disease link to developmental hypoxia. *Circulation* **144**, 1429-1443. doi:10.1161/CIRCULATIONAHA.121.054689

Gopel, T. and Burggren, W. W. (2024). Temperature and hypoxia trigger developmental phenotypic plasticity of cardiorespiratory physiology and growth in the parthenogenetic marbled crayfish, *Procambarus virginalis* Lyko, 2017. *Comp. Biochem. Physiol. A Mol. Integr. Physiol.* **288**, 111562. doi:10.1016/j.cbpa.2023.111562

Guski, H., Meerson, F. Z. and Wassilew, G. (1981). Comparative study of ultrastructure and function of the rat heart hypertrophied by exercise or hypoxia. *Exp. Pathol.* **20**, 108-120. doi:10.1016/S0232-1513(81)80018-7

Hanson, M. A., Gluckman, P. D. and Godfrey, K. M. (2014). Developmental epigenetics and risks of later non-communicable disease. In *Hormones, Intrauterine Health, and Programming*, Vol. 12 (ed. J. R. Seckl and Y. Christen), pp. 175-183: Springer.

Hautefort, A., Mendes-Ferreira, P., Sabourin, J., Manaud, G., Bertero, T., Rucker-Martin, C., Riou, M., Adao, R., Manoury, B., Lambert, M. et al. (2019). bmpr2 mutant rats develop pulmonary and cardiac characteristics of pulmonary arterial hypertension. *Circulation* **139**, 932-948. doi:10.1161/CIRCULATIONAHA.118.033744

Ho, D. H. and Burggren, W. W. (2012). Parental hypoxic exposure confers offspring hypoxia resistance in zebrafish (*Danio rerio*). *J. Exp. Biol.* **215**, 4208-4216. doi:10.1242/jeb.074781

Itani, N., Salinas, C. E., Villena, M., Skeffington, K. L., Beck, C., Villamor, E., Blanco, C. E. and Giussani, D. A. (2018). The highs and lows of programmed cardiovascular disease by developmental hypoxia: studies in the chicken embryo. *J. Physiol.* **596**, 2991-3006. doi:10.1113/JP274111

Jackson, D. C. (1987). Cardiovascular function in turtles during anoxia and acidosis: *in-vivo* and *in-vitro* studies. *Am. Zool.* **27**, 49-58. doi:10.1093/icb/27.1.49

Jackson, D. C. (2000). Living without oxygen: lessons from the freshwater turtle. *Comp. Biochem. Physiol. A Mol. Integr. Physiol.* **125**, 299-315. doi:10.1016/S1095-6433(00)00160-4

Jackson, D. C. and Silverblatt, H. (1974). Respiration and acid-base status of turtles following experimental dives. *Am. J. Physiol.* **226**, 903-909. doi:10.1152/ajplegacy.1974.226.4.903

James-Kracke, M. R. (1992). Quick and accurate method to convert BCECF fluorescence to pH_i: calibration in three different types of cell preparations. *J. Cell. Physiol.* **151**, 596-603. doi:10.1002/jcp.1041510320
Kam, Y. C. (1993). Physiological effects of hypoxia on metabolism and growth of turtle embryos. *Respir. Physiol.* **92**, 127-138. doi:10.1016/0034-5687(93)90033-7
Kao, Y. H., Chen, Y. C., Cheng, C. C., Lee, T. I., Chen, Y. J. and Chen, S. A. (2010). Tumor necrosis factor-alpha decreases sarcoplasmic reticulum Ca^{2+}-ATPase expressions via the promoter methylation in cardiomyocytes. *Crit. Care Med.* **38**, 217-222. doi:10.1097/CCM.0b013e3181b4a854
Keen, J. E., Farrell, A. P., Tibbits, G. F. and Brill, R. W. (1992). Cardiac physiology in tunas. II. Effect of ryanodine, calcium, and adrenaline on force-frequency relationships in atrial strips from skipjack tuna, *Katsuwonus pelamis*. *Can. J. Zool.* **70**, 1211-1217. doi:10.1139/z92-168
Klaiman, J. M., Pyle, W. G. and Gillis, T. E. (2014). Cold acclimation increases cardiac myofilament function and ventricular pressure generation in trout. *J. Exp. Biol.* **217**, 4132-4140. doi:10.1242/jeb.109041
Kubly, K. L. and Stecyk, J. A. W. (2019). Contractile performance of the Alaska blackfish (*Dallia pectoralis*) ventricle: Assessment of the effects of temperature, pacing frequency, the role of the sarcoplasmic reticulum in contraction and adrenergic stimulation. *Comp. Biochem. Physiol. A Mol. Integr. Physiol.* **238**, 110564. doi:10.1016/j.cbpa.2019.110564
Lattanzio, F. A., Jr (1990). The effects of pH and temperature on fluorescent calcium indicators as determined with Chelex-100 and EDTA buffer systems. *Biochem. Biophys. Res. Commun.* **171**, 102-108. doi:10.1016/0006-291X(90)91362-V
Lillywhite, H. B., Zippel, K. C. and Farrell, A. P. (1999). Resting and maximal heart rates in ectothermic vertebrates. *Comp. Biochem. Physiol. A Mol. Integr. Physiol.* **124**, 369-382. doi:10.1016/S1095-6433(99)00129-4
MacCormack, T. J., Treberg, J. R., Almeida-Val, V. M., Val, A. L. and Driedzic, W. R. (2003). Mitochondrial K_{ATP} channels and sarcoplasmic reticulum influence cardiac force development under anoxia in the Amazonian armored catfish, *Liposarcus pardalis*. *Comp. Biochem. Physiol. A Mol. Integr. Physiol.* **134**, 441-448. doi:10.1016/S1095-6433(02)00315-X
Mackrill, J. J. (2010). Ryanodine-receptor calcium channels and their partners as drug targets. *Biochem. Pharmacol.* **79**, 1535-1543. doi:10.1016/j.bcp.2010.01.014
Marston, S. (2018). The molecular mechanisms of mutations in actin and myosin that cause inherited myopathy. *Int. J. Mol. Sci.* **19**, 2020. doi:10.3390/ijms19072020
Massey, M. D. and Dalziel, A. C. (2023). Parental early life environments drive transgenerational plasticity of offspring metabolism in a freshwater fish (*Danio rerio*). *Biol. Lett.* **19**, 20230266. doi:10.1098/rsbl.2023.0266
Meyer, J. N., Smith, J. D., Winston, G. W. and Di Giulio, R. T. (2003). Antioxidant defenses in killifish (*Fundulus heteroclitus*) exposed to contaminated sediments and model prooxidants: short-term and heritable responses. *Aquat Toxicol.* **65**, 377-395. doi:10.1016/j.aquatox.2003.06.001
Moczek, A. P. (2015). Developmental plasticity and evolution – quo vadis? *Heredity* **115**, 302-305. doi:10.1038/hdy.2015.14
Morciano, G., Bonora, M., Campo, G., Aquila, G., Rizzo, P., Giorgi, C., Wieckowski, M. R. and Pinton, P. (2017). Mechanistic role of mPTP in ischemia-reperfusion injury. *Adv. Exp. Med. Biol.* **982**, 169-189. doi:10.1007/978-3-319-55330-6_9
Munkittrick, K. R. and Dixon, D. G. (1988). Evidence for a maternal yolk factor associated with increased tolerance and resistance of feral white sucker (*Catostomus commersoni*) to waterborne copper. *Ecotoxicol. Environ. Saf.* **15**, 7-20. doi:10.1016/0147-6513(88)90038-3
Murphy, E. and Steenbergen, C. (2008). Mechanisms underlying acute protection from cardiac ischemia-reperfusion injury. *Physiol. Rev.* **88**, 581-609. doi:10.1152/physrev.00024.2007
Oda, T., Yang, Y., Uchinoumi, H., Thomas, D. D., Chen-Izu, Y., Kato, T., Yamamoto, T., Yano, M., Cornea, R. L. and Bers, D. M. (2015). Oxidation of ryanodine receptor (RyR) and calmodulin enhance Ca^{2+} release and pathologically alter, RyR structure, and calmodulin affinity. *J. Mol. Cell. Cardiol.* **85**, 240-248. doi:10.1016/j.yjmcc.2015.06.009
Onishi, J., Browne, V. A., Kono, S., Stiffel, V. M. and Gilbert, R. D. (2004). Effects of long-term, high-altitude hypoxia and troponin-I phosphorylation on cardiac myofilament calcium responses in fetal and nonpregnant sheep. *J. Soc. Gynecol. Investig.* **11**, 1-8. doi:10.1016/j.jsgi.2003.07.003
Orchard, C. H. and Kentish, J. C. (1990). Effects of changes of pH on the contractile function of cardiac muscle. *Am. J. Physiol. Cell Physiol.* **258**, C967-C981. doi:10.1152/ajpcell.1990.258.6.C967
Overgaard, J., Stecyk, J. A., Farrell, A. P. and Wang, T. (2002). Adrenergic control of the cardiovascular system in the turtle *Trachemys scripta*. *J. Exp. Biol.* **205**, 3335-3345. doi:10.1242/jeb.205.21.3335
Pan, T. C. and Burggren, W. W. (2013). Ontogeny of hypoxic modulation of cardiac performance and its allometry in the African clawed frog, *Xenopus laevis*. *J. Comp. Physiol. B* **183**, 123-133. doi:10.1007/s00360-012-0686-3
Peyronnet, J., Dalmaz, Y., Ehrstrom, M., Mamet, J., Roux, J. C., Pequignot, J. M., Thoren, H. P. and Lagercrantz, H. (2002). Long-lasting adverse effects of prenatal hypoxia on developing autonomic nervous system and cardiovascular parameters in rats. *Pflügers Archiv.* **443**, 858-865. doi:10.1007/s00424-001-0766-9
Rabkin, S. W. and Wong, C. N. (2023). Epigenetics in heart failure: role of DNA methylation in potential pathways leading to heart failure with preserved ejection fraction. *Biomedicines* **11**, jeb205419. doi:10.3390/biomedicines11102815
Robertson, C. E., Wright, P. A., Koblitz, L. and Bernier, N. J. (2014). Hypoxia-inducible factor-1 mediates adaptive developmental plasticity of hypoxia tolerance in zebrafish, *Danio rerio*. *Proc. Biol. Sci.* **281**, 20140637.
Ronkainen, V. P., Skoumal, R. and Tavi, P. (2011). Hypoxia and HIF-1 suppress SERCA2a expression in embryonic cardiac myocytes through two interdependent hypoxia response elements. *J. Mol. Cell. Cardiol.* **50**, 1008-1016. doi:10.1016/j.yjmcc.2011.02.017
Ruhr, I. M., McCourty, H., Bajjig, A., Crossley, D. A., Shiels, I. I. and Galli, H. A. (2019). Developmental plasticity of cardiac anoxia-tolerance in juvenile common snapping turtles (*Chelydra serpentina*). *Proc. Biol. Sci.* **286**, 20191072.
Ruhr, I. M., Bierstedt, J., Rhen, T., Das, D., Singh, S. K., Miller, S., Crossley, D. A. and Galli, I. I. (2021). Developmental programming of DNA methylation and gene-expression patterns is associated with extreme cardiovascular tolerance to anoxia in the common snapping turtle. *Epigenetics Chromatin* **14**, 42. doi:10.1186/s13072-021-00414-7
Sartori, M. R., Kohl, Z. F., Taylor, E. W., Abe, A. S. and Crossley, D. A., II (2019). Blood flow distribution in embryonic common snapping turtles, *Chelydra serpentina* (Reptilia; Chelonia), during acute hypoxia and α-adrenergic regulation. *Comp. Biochem. Physiol. A Mol. Integr. Physiol.* **238**, 110575. doi:10.1016/j.cbpa.2019.110575
Satoh, K., Nigro, P., Zeidan, A., Soe, N. N., Jaffre, F., Oikawa, M., O'Dell, M. R., Cui, Z., Menon, P., Lu, Y. et al. (2011). Cyclophilin A promotes cardiac hypertrophy in apolipoprotein E-deficient mice. *Arterioscler. Thromb. Vasc. Biol.* **31**, 1116-1123. doi:10.1161/ATVBAHA.110.214601
Schaper, J., Hehrlein, F., Schlepper, M. and Thiedemann, K. U. (1977). Ultrastructural alterations during ischemia and reperfusion in human hearts during cardiac surgery. *J. Mol. Cell. Cardiol.* **9**, 175-189. doi:10.1016/0022-2828(77)90028-1
Shiels, H. A. and Galli, G. L. J. (2014). The sarcoplasmic reticulum and the evolution of the vertebrate heart. *Physiol* **29**, 456-469. doi:10.1152/physiol.00015.2014
Shiels, H. and Farrell, A. P. (1997). The effect of temperature and adrenaline on the relative importance of the sarcoplasmic reticulum in contributing Ca^{2+} to force development in isolated ventricular trabeculae from rainbow trout. *J. Exp. Biol.* **200**, 1607-1621. doi:10.1242/jeb.200.11.1607
Shiels, H. A. and Farrell, A. P. (2000). The effect of ryanodine on isometric tension development in isolated ventricular trabeculae from Pacific mackerel (*Scomber japonicus*). *Comp. Biochem. Physiol. A Mol. Integr. Physiol.* **125**, 331-341. doi:10.1016/S1095-6433(00)00161-6
Shiels, H. A., Freund, E. V., Farrell, A. P. and Block, B. A. (1999). The sarcoplasmic reticulum plays a major role in isometric contraction in atrial muscle of yellowfin tuna. *J. Exp. Biol.* **202**, 881-890. doi:10.1242/jeb.202.7.881
Shiels, H. A., Di Maio, A., Thompson, S. and Block, B. A. (2011). Warm fish with cold hearts: thermal plasticity of excitation-contraction coupling in bluefin tuna. *Proc. Biol. Sci.* **278**, 18-27.
Shiels, H. A., Vornanen, M. and Farrell, A. P. (2002a). Effects of temperature on intracellular $[Ca^{2+}]$ in trout atrial myocytes. *J. Exp. Biol.* **205**, 3641-3650. doi:10.1242/jeb.205.23.3641
Shiels, H. A., Vornanen, M. and Farrell, A. P. (2002b). The force-frequency relationship in fish hearts - a review. *Comp. Biochem. Physiol. A Mol. Integr. Physiol.* **132**, 811-826. doi:10.1016/S1095-6433(02)00050-8
Smith, B., Crossley, J. L., Elsey, R. M., Hicks, J. W. and Crossley, D. A., II (2019). Embryonic developmental oxygen preconditions cardiovascular functional response to acute hypoxic exposure and maximal beta-adrenergic stimulation of anesthetized juvenile American alligators (*Alligator mississippiensis*). *J. Exp. Biol.* **222**, jeb205419. doi:10.1242/jeb.205419
Smith, B., Crossley, D. A., , II, Wang, T. and Joyce, W. (2022). No evidence for pericardial restraint in the snapping turtle (*Chelydra serpentina*) following pharmacologically induced bradycardia at rest or during exercise. *Am. J. Physiol. Regul. Integr. Comp. Physiol.* **322**, R389-R399. doi:10.1152/ajpregu.00004.2022
Stecyk, J. A. W. and Farrell, A. P. (2007). Effects of extracellular changes on spontaneous heart rate of normoxia- and anoxia-acclimated turtles (*Trachemys scripta*). *J. Exp. Biol.* **210**, 421-431. doi:10.1242/jeb.02653
Stecyk, J. A. W., Bock, C., Overgaard, J., Wang, T., Farrell, A. P. and Portner, H. O. (2009). Correlation of cardiac performance with cellular energetic components in the oxygen-deprived turtle heart. *Am. J. Physiol. Regul. Integr. Comp. Physiol.* **297**, R756-R768. doi:10.1152/ajpregu.00102.2009
Sumandea, M. P. and Steinberg, S. F. (2011). Redox signaling and cardiac sarcomeres. *J. Biol. Chem.* **286**, 9921-9927. doi:10.1074/jbc.R110.175489
Tate, K. B., Kohl, Z. F., Eme, J., Rhen, T. and Crossley, D. A., II. (2015). Critical windows of cardiovascular susceptibility to developmental hypoxia in common snapping turtle (*Chelydra serpentina*) embryos. *Physiol. Biochem. Zool.* **88**, 103-115. doi:10.1086/677683
Tibbits, G. F., Kashihara, H., Thomas, M. J., Keen, J. E. and Farrell, A. P. (1990). Ca^{2+} transport in myocardial sarcolemma from rainbow trout. *Am. J. Physiol. Regul. Integr. Comp. Physiol.* **259**, R453-R460. doi:10.1152/ajpregu.1990.259.3.R453

Torres, R. F. and Kerr, B. (2021). Spatial learning is associated with antagonist outcomes for DNA methylation and DNA hydroxymethylation in the transcriptional regulation of the ryanodine receptor 3. *Neural Plast.* **2021**, 9930962. doi:10.1155/2021/9930962

Tsai, C. T., Wu, C. K., Lee, J. K., Chang, S. N., Kuo, Y. M., Wang, Y. C., Lai, L. P., Chiang, F. T., Hwang, J. J. and Lin, J. L. (2015). TNF-alpha down-regulates sarcoplasmic reticulum Ca^{2+}-ATPase expression and leads to left ventricular diastolic dysfunction through binding of NF-kappaβ to promoter-response element. *Cardiovasc. Res.* **105**, 318-329. doi:10.1093/cvr/cvv008

Ultsch, G. R. (2006). The ecology of overwintering among turtles: where turtles overwinter and its consequences. *Biol. Rev.* **81**, 339-367. doi:10.1017/S1464793106007032

Umbarkar, P., Singh, A. P., Gupte, M., Verma, V. K., Galindo, C. L., Guo, Y., Zhang, Q., McNamara, J. W., Force, T. and Lal, H. (2019). Cardiomyocyte SMAD4-dependent TGF-beta signaling is essential to Mmaintain adult heart homeostasis. *JACC Basic Transl. Sci.* **4**, 41-53. doi:10.1016/j.jacbts.2018.10.003

Villamor, E., Kessels, C. G., Ruijtenbeek, K., van Suylen, R. J., Belik, J., de Mey, J. G. and Blanco, C. E. (2004). Chronic in ovo hypoxia decreases pulmonary arterial contractile reactivity and induces biventricular cardiac enlargement in the chicken embryo. *Am. J. Physiol. Regul. Integr. Comp. Physiol.* **287**, R642-R651. doi:10.1152/ajpregu.00611.2003

Vornanen, M., Shiels, H. A. and Farrell, A. P. (2002). Plasticity of excitation-contraction coupling in fish cardiac myocytes. *Comp. Biochem. Physiol. A Mol. Integr. Physiol.* **132**, 827-846. doi:10.1016/S1095-6433(02)00051-X

Warren, D. E. and Jackson, D. C. (2007). Effects of temperature on anoxic submergence: skeletal buffering, lactate distribution, and glycogen utilization in the turtle, *Trachemys scripta*. *Am. J. Physiol. Regul. Integr. Comp. Physiol.* **293**, R458-R467. doi:10.1152/ajpregu.00174.2006

Wasser, J. S., Guthrie, S. S. and Chari, M. (1997). *In-vitro* tolerance to anoxia and ischemia in isolated hearts from hypoxia-sensitive and hypoxia-tolerant turtles. *Comp. Biochem. Physiol. A Mol. Integr. Physiol.* **118**, 1359-1370. doi:10.1016/S0300-9629(97)00248-X

Wasser, J. S., Meinertz, E. A., Chang, S. Y., Lawler, R. G. and Jackson, D. C. (1992). Metabolic and cardiodynamic responses of isolated turtle hearts to ischemia and reperfusion. *Am. J. Physiol. Regul. Integr. Comp. Physiol.* **262**, R437-R443. doi:10.1152/ajpregu.1992.262.3.R437

Wearing, O. H., Conner, J., Nelson, D., Crossley, J. and Crossley, D. A., II. (2017). Embryonic hypoxia programmes postprandial cardiovascular function in adult common snapping turtles (*Chelydra serpentina*). *J. Exp. Biol.* **220**, 2589-2597. doi:10.1242/jeb.160549

Wearing, O. H., Eme, J., Rhen, T. and Crossley, D. A., II. (2016). Phenotypic plasticity in the common snapping turtle (*Chelydra serpentina*): long-term physiological effects of chronic hypoxia during embryonic development. *Am. J. Physiol. Regul. Integr. Comp. Physiol.* **310**, R176-R184. doi:10.1152/ajpregu.00293.2015

Williams, A. L., Walton, C. B., MacCannell, K. A., Avelar, A. and Shohet, R. V. (2019). HIF-1 regulation of miR-29c impairs SERCA2 expression and cardiac contractility. *Am. J. Physiol. Heart Circ. Physiol.* **316**, H554-H565. doi:10.1152/ajpheart.00617.2018

Wu, R. S. S. (2009). Effects of hypoxia on fish reproduction and development. In *Fish Physiology: Hypoxia*, Vol. 27 (ed. J. G. Richards, A. P. Farrell and C. J. Brauner), pp. 79-141. Oxford, U.K: Academic Press.

Xu, Y., Liu, L., Pan, B., Zhu, J., Nan, C., Huang, X. and Tian, J. (2015). DNA methylation regulates mouse cardiac myofibril gene expression during heart development. *J. Biomed. Sci.* **22**, 88. doi:10.1186/s12929-015-0203-6

Yntema, C. L. (1968). A series of stages in the embryonic development of *Chelydra serpentina*. *J. Morphol.* **125**, 219-251. doi:10.1002/jmor.1051250207